TABLE 1. Summary of Clinical Features of 79 Patients With *ABCA4*-Related Retinal Disease

Median age of onset, y (range)		22.0 (5–71)
Median age at examination, y (range)		40.0 (15–79)
Median duration of disease, y (range)		10.0 (0–54)
LogMAR visual acuity (range)	R	1.00 (−0.08–1.78)
	L	1.00 (−0.08–4.00)
AF subtype, $n = 71$	1	$n = 21$
	2	$n = 34$
	3	$n = 16$
ERG group, $n = 70$	1	$n = 34$
	2	$n = 7$
	3	$n = 29$

AF, autofluorescence; ERG, electroretinography; R, right eye; L, left eye.

novel NGS strategy for *ABCA4* screening in a large, well-characterized British cohort of patients with likely *ABCA4*-associated phenotypes and report novel disease-causing variants.

MATERIALS AND METHODS

Patients

Prescreening with APEX technology was performed in a cohort of 232 patients seen at Moorfields Eye Hospital with a clinical diagnosis of retinopathy compatible with *ABCA4*-associated retinal disease. Two or more variants were identified in 103 patients, one variant in 79 subjects, and no variants in 50 individuals. The 79 patients with only one *ABCA4* allele were recruited for this study. After informed consent was obtained, blood samples were taken from all individuals for NGS of *ABCA4*. The protocol of the study adhered to the provisions of the Declaration of Helsinki and was approved by the Ethics Committee of Moorfields Eye Hospital. The age at onset was defined as the age at which visual loss was first noted by the patient. The duration of

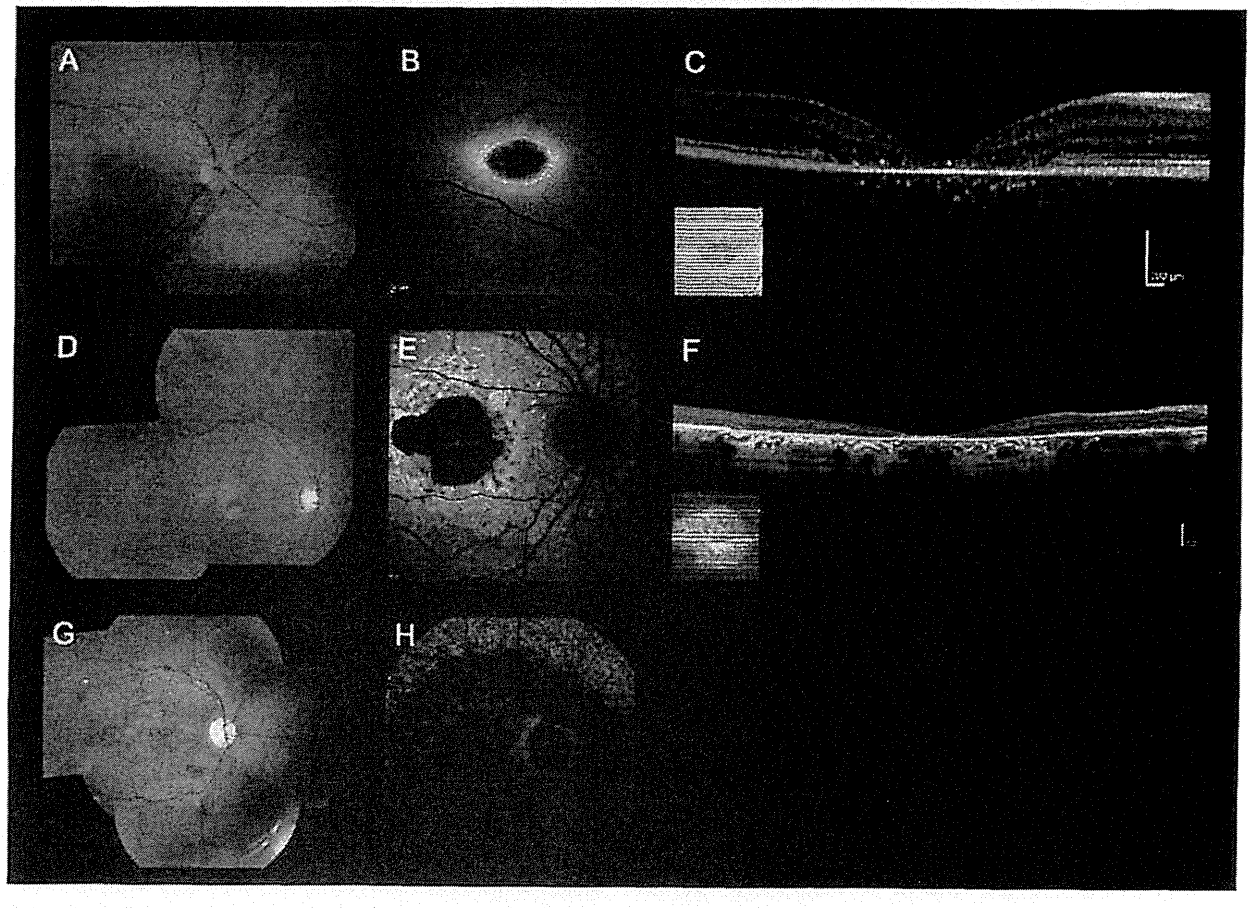

FIGURE 1. Color fundus photographs, autofluorescence images, and optical coherence tomography of three representative cases harboring two or more *ABCA4* variants with "typical" *ABCA4*-associated retinal disease (patients 19, 36, and 17). Color fundus photograph of patient 19 shows macular atrophy (A) and AF imaging demonstrates a localized low AF signal at the fovea, with a high signal edge surrounded by a homogeneous background (B). SD-OCT demonstrates marked outer retinal loss at the central macula (C). Patient 36 has macular atrophy surrounded by numerous yellow-white flecks (D) and a localized low AF signal at the macula surrounded by a heterogeneous background, with peripapillary sparing (E). Generalized loss of outer retinal architecture is seen on SD-OCT. Patient 17 has widespread multiple areas of atrophy with patchy pigmentation (G) and multiple areas of low AF signal at the posterior pole with a heterogeneous background (H).

ABCA4 Gene Screening by Next-Generation Sequencing in a British Cohort

Kaoru Fujinami,[1-4] Jana Zernant,[5] Ravinder K. Chana,[3,4] Genevieve A. Wright,[3,4] Kazushige Tsunoda,[1] Yoko Ozawa,[2] Kazuo Tsubota,[2] Andrew R. Webster,[3,4] Anthony T. Moore,[3,4] Rando Allikmets,[5,6] and Michel Michaelides[3,4]

[1]Laboratory of Visual Physiology, National Institute of Sensory Organs, National Tokyo Medical Center, Tokyo, Japan
[2]Department of Ophthalmology, Keio University, School of Medicine, Tokyo, Japan
[3]UCL Institute of Ophthalmology, London, United Kingdom
[4]Moorfields Eye Hospital, London, United Kingdom
[5]Department of Ophthalmology, Columbia University, New York, New York
[6]Department of Pathology and Cell Biology, Columbia University, New York, New York

Correspondence: Rando Allikmets, Columbia University, 630 West 168th Street, New York, NY 10032; rla22@columbia.edu.
Michel Michaelides, UCL Institute of Ophthalmology, 11-43 Bath Street, London, EC1V 9EL, UK; michel.michaelides@ucl.ac.uk.

Submitted: June 9, 2013
Accepted: August 19, 2013

Citation: Fujinami K, Zernant J, Chana RK, et al. *ABCA4* gene screening by next-generation sequencing in a British cohort. *Invest Ophthalmol Vis Sci.* 2013;54:6662-6674. DOI:10.1167/iovs.13-12570

Purpose. We applied a recently reported next-generation sequencing (NGS) strategy for screening the *ABCA4* gene in a British cohort with *ABCA4*-associated disease and report novel mutations.

Methods. We identified 79 patients with a clinical diagnosis of *ABCA4*-associated disease who had a single variant identified by the *ABCA4* microarray. Comprehensive phenotypic data were obtained, and the NGS strategy was applied to identify the second allele by means of sequencing the entire coding region and adjacent intronic sequences of the *ABCA4* gene. Identified variants were confirmed by Sanger sequencing and assessed for pathogenicity by in silico analysis.

Results. Of the 42 variants detected by prescreening with the microarray, in silico analysis suggested that 34, found in 66 subjects, were disease-causing and 8, found in 13 subjects, were benign variants. We detected 42 variants by NGS, of which 39 were classified as disease-causing. Of these 39 variants, 31 were novel, including 16 missense, 7 splice-site-altering, 4 nonsense, 1 in-frame deletion, and 3 frameshift variants. Two or more disease-causing variants were confirmed in 37 (47%) of 79 patients, one disease-causing variant in 36 (46%) subjects, and no disease-causing variant in 6 (7%) individuals.

Conclusions. Application of the NGS platform for *ABCA4* screening enabled detection of the second disease-associated allele in approximately half of the patients in a British cohort where one mutation had been detected with the arrayed primer extension (APEX) array. The time- and cost-efficient NGS strategy is useful in screening large cohorts, which will be increasingly valuable with the advent of *ABCA4*-directed therapies.

Keywords: ABCA4, next generation sequencing, Stargardt disease

Stargardt disease is the most common form of inherited macular dystrophy and is caused by recessive mutations in the *ABCA4* gene.[1,2] Stargardt disease typically presents with central macular atrophy and yellow-white flecks at the posterior pole, primarily at the level of the RPE.[2,3] A highly variable phenotype and progression of Stargardt disease have been documented, and mutations in *ABCA4* also have been implicated in cone dystrophy, cone-rod dystrophy, and "retinitis pigmentosa."[4-12] In this report, we will use the term "*ABCA4*-associated retinal disease" to refer to the broad range and variability of clinical manifestations of retinopathy due to *ABCA4* variants.

The carrier frequency of likely pathogenic *ABCA4* alleles has been reported to be as high as 1:20[13,14] and more than 700 *ABCA4* variants have been identified so far.[1,2,5-29] The high allelic heterogeneity makes molecular genetic analyses of *ABCA4*-associated retinal disease very challenging. It has been reported that direct Sanger sequencing of the entire *ABCA4* coding region (50 exons) detects between 66% and 80% of disease-causing alleles[13,21]; however, this approach has significant limitations in large patient cohorts due to the prohibitive time and cost implications.[3,5]

Since the development of the *ABCA4* genotyping microarray, using arrayed primer extension (APEX) technology,[14] systematic screening of all known previously reported *ABCA4* variants has been available[26,30]; APEX detects approximately 65% to 75% of all disease-associated alleles. However, by definition, novel variants are not detected by APEX technology, necessitating the use of other methodologies for high-throughput systematic screening of the entire coding region, especially in cases where one or both disease-causing alleles have failed to be identified by the array.

Zernant et al. recently reported the capability of a next-generation sequencing (NGS) strategy to detect new *ABCA4* variants that were not included on the APEX array; all 50 *ABCA4* exons of 168 patients were amplified in parallel using an amplicon tagging PCR protocol and NGS was applied to the resulting amplicons.[5] The purpose of this study was to apply this

Copyright 2013 The Association for Research in Vision and Ophthalmology, Inc.

22. Maeda T, Maeda A, Matosky M, et al. Evaluation of potential therapies for a mouse model of human age-related macular degeneration caused by delayed all-trans-retinal clearance. *Invest Ophthalmol Vis Sci.* 2009;50:4917–4925.
23. Okano K, Maeda A, Chen Y, et al. Retinal cone and rod photoreceptor cells exhibit differential susceptibility to light-induced damage. *J Neurochem.* 2012;121:146–156.
24. Chen Y, Okano K, Maeda T, et al. Mechanism of all-trans-retinal toxicity with implications for Stargardt disease and age-related macular degeneration. *J Biol Chem.* 2012;287:5059–5069.
25. Mata NL, Weng J, Travis GH. Biosynthesis of a major lipofuscin fluorophore in mice and humans with ABCR-mediated retinal and macular degeneration. *Proc Natl Acad Sci U S A.* 2000;97:7154–7159.
26. Sparrow JR, Gregory-Roberts E, Yamamoto K, et al. The bisretinoids of retinal pigment epithelium. *Prog Retin Eye Res.* 2012;31:121–135.
27. Sparrow JR, Nakanishi K, Parish CA. The lipofuscin fluorophore A2E mediates blue light-induced damage to retinal pigmented epithelial cells. *Invest Ophthalmol Vis Sci.* 2000;41:1981–1989.
28. Dorey CK, Wu G, Ebenstein D, Garsd A, Weiter JJ. Cell loss in the aging retina. Relationship to lipofuscin accumulation and macular degeneration. *Invest Ophthalmol Vis Sci.* 1989;30:1691–1699.
29. von Ruckmann A, Fitzke FW, Bird AC. Distribution of fundus autofluorescence with a scanning laser ophthalmoscope. *Br J Ophthalmol.* 1995;79:407–412.
30. Chen B, Tosha C, Gorin MB, Nusinowitz S. Analysis of autofluorescent retinal images and measurement of atrophic lesion growth in Stargardt disease. *Exp Eye Res.* 2010;91:143–152.
31. Fishman GA, Stone EM, Grover S, Derlacki DJ, Haines HL, Hockey RR. Variation of clinical expression in patients with Stargardt dystrophy and sequence variations in the ABCR gene. *Arch Ophthalmol.* 1999;117:504–510.
32. Burke TR, Tsang SH. Allelic and phenotypic heterogeneity in ABCA4 mutations. *Ophthalmic Genet.* 2011;32:165–174.
33. Zernant J, Schubert C, Im KM, et al. Analysis of the ABCA4 gene by next-generation sequencing. *Invest Ophthalmol Vis Sci.* 2011;52:8479–8487.
34. Allikmets R. A photoreceptor cell-specific ATP-binding transporter gene (ABCR) is mutated in recessive Stargardt macular dystrophy. *Nat Genet.* 1997;17:122.
35. Rozet JM, Gerber S, Souied E, et al. Spectrum of ABCR gene mutations in autosomal recessive macular dystrophies. *Eur J Hum Genet.* 1998;6:291–295.
36. Lewis RA, Shroyer NF, Singh N, et al. Genotype/phenotype analysis of a photoreceptor-specific ATP-binding cassette transporter gene, ABCR, in Stargardt disease. *Am J Hum Genet.* 1999;64:422–434.
37. Maugeri A, Klevering BJ, Rohrschneider K, et al. Mutations in the ABCA4 (ABCR) gene are the major cause of autosomal recessive cone-rod dystrophy. *Am J Hum Genet.* 2000;67:960–966.
38. Papaioannou M, Ocaka L, Bessant D, et al. An analysis of ABCR mutations in British patients with recessive retinal dystrophies. *Invest Ophthalmol Vis Sci.* 2000;41:16–19.
39. Rivera A, White K, Stohr H, et al. A comprehensive survey of sequence variation in the ABCA4 (ABCR) gene in Stargardt disease and age-related macular degeneration. *Am J Hum Genet.* 2000;67:800–813.
40. Birch DG, Peters AY, Locke KL, Spencer R, Megarity CF, Travis GH. Visual function in patients with cone-rod dystrophy (CRD) associated with mutations in the ABCA4(ABCR) gene. *Exp Eye Res.* 2001;73:877–886.
41. Briggs CE, Rucinski D, Rosenfeld PJ, Hirose T, Berson EL, Dryja TP. Mutations in ABCR (ABCA4) in patients with Stargardt macular degeneration or cone-rod degeneration. *Invest Ophthalmol Vis Sci.* 2001;42:2229–2236.
42. Fumagalli A, Ferrari M, Soriani N, et al. Mutational scanning of the ABCR gene with double-gradient denaturing-gradient gel electrophoresis (DG-DGGE) in Italian Stargardt disease patients. *Hum Genet.* 2001;109:326–338.
43. Shroyer NF, Lewis RA, Yatsenko AN, Wensel TG, Lupski JR. Cosegregation and functional analysis of mutant ABCR (ABCA4) alleles in families that manifest Stargardt disease and age-related macular degeneration. *Hum Mol Genet.* 2001;10:2671–2678.
44. Webster AR, Heon E, Lotery AJ, et al. An analysis of allelic variation in the ABCA4 gene. *Invest Ophthalmol Vis Sci.* 2001;42:1179–1189.
45. Lange C, Feltgen N, Junker B, Schulze-Bonsel K, Bach M. Resolving the clinical acuity categories "hand motion" and "counting fingers" using the Freiburg Visual Acuity Test (FrACT). *Graefes Arch Clin Exp Ophthalmol.* 2009;247:137–142.
46. Robson AG, Tufail A, Fitzke F, et al. Serial imaging and structure-function correlates of high-density rings of fundus autofluorescence in retinitis pigmentosa. *Retina.* 2011;31:1670–1679.
47. Bellmann C, Rubin GS, Kabanarou SA, Bird AC, Fitzke FW. Fundus autofluorescence imaging compared to different confocal scanning laser ophthalmoscopes. *Br J Ophthalmol.* 2003;87:1381–1386.
48. Robson AG, Egan CA, Luong VA, Bird AC, Holder GE, Fitzke FW. Comparison of fundus autofluorescence with photopic and scotopic fine-matrix mapping in patients with retinitis pigmentosa and normal visual acuity. *Invest Ophthalmol Vis Sci.* 2004;45:4119–4125.
49. Sergouniotis PI, Davidson AE, Lenassi E, Devery SR, Moore AT, Webster AR. Retinal structure, function, and molecular pathologic features in gyrate atrophy. *Ophthalmology.* 2012;119:596–605.
50. Orita M, Iwahana H, Kanazawa H, Hayashi K, Sekiya T. Detection of polymorphisms of human DNA by gel electrophoresis as single-strand conformation polymorphisms. *Proc Natl Acad Sci U S A.* 1989;86:2766–2770.
51. Jaakson K, Zernant J, Kulm M, et al. Genotyping microarray (gene chip) for the ABCR (ABCA4) gene. *Hum Mutat.* 2003;22:395–403.
52. Ng PC, Henikoff S. SIFT: predicting amino acid changes that affect protein function. *Nucleic Acids Res.* 2003;31:3812–3814.
53. Adzhubei IA, Schmidt S, Peshkin L, et al. A method and server for predicting damaging missense mutations. *Nat Methods.* 2010;7:248–249.
54. Sodi A, Bini A, Passerini I, Forconi S, Menchini U, Torricelli F. Different patterns of fundus autofluorescence related to ABCA4 gene mutations in Stargardt disease. *Ophthalmic Surg Lasers Imaging.* 2010;41:48–53.
55. Klevering BJ, Yzer S, Rohrschneider K, et al. Microarray-based mutation analysis of the ABCA4 (ABCR) gene in autosomal recessive cone-rod dystrophy and retinitis pigmentosa. *Eur J Hum Genet.* 2004;12:1024–1032.
56. Schindler EI, Nylen EL, Ko AC, et al. Deducing the pathogenic contribution of recessive ABCA4 alleles in an outbred population. *Hum Mol Genet.* 2010;19:3693–3701.
57. Cella W, Greenstein VC, Zernant-Rajang J, et al. G1961E mutant allele in the Stargardt disease gene ABCA4 causes bull's eye maculopathy. *Exp Eye Res.* 2009;89:16–24.
58. Fujinami K, Zernant J, Chana RK, et al. ABCA4 gene screening by next-generation sequencing in a British cohort. *Invest Ophthalmol Vis Sci.* 2013;54:6662–6674.

agreement in atrophy measurement. Software, which defines and calculates the atrophic lesions automatically, may arguably be more reliable in performing quantitative analysis, although this also is not without its limitations. Many of the older AF images at baseline in our study could not be analyzed with such recent software. Quantitative analysis of optical coherence tomography data also will have an important role in future studies of atrophy progression. In addition, wide-field AF imaging systems also may aid a more comprehensive assessment in terms of AF type classification (less atrophic lesions "beyond the scope" of the acquired image) and quantitative atrophy measurement.

Two different gene screening methods (SSCP and microarray) were applied in our cohort due to the technological advances made during the period of this study. In keeping with previous studies, we were able to undertake segregation analysis in a limited number of cases due to the unavailability of other family samples. Undoubtedly, more advanced recent mutation analysis, such as PCR enrichment-based next-generation sequencing (NGS), will result in a higher mutation detection rate, including identifying the often "missing" second *ABCA4* allele, which will allow more informed genotype–phenotype correlations to be investigated.[33,58] The genotype–phenotype correlations have been investigated by comparing the *ABCA4* gene mutations with the clinical features in this study; however, it is likely that other factors must be considered, including environmental, genetic, and epigenetic modifiers.

This study has investigated AF subtypes/patterns in a longitudinal survey, and determined changes in AF pattern and progression of atrophy. It has highlighted that patients with localized foveal atrophy tend to experience milder progression, including milder visual acuity loss, whereas those subjects with multiple large areas of retinal atrophy had severe progression and severe visual acuity reduction. These data assist counselling with regard to visual prognosis, and may help in study design and patient selection of clinical trials for *ABCA4*-related retinopathy.

Acknowledgments

The authors thank Graham E. Holder, Antony G. Robson, Alice E. Davidson, Panagiotis I. Sergouniotis, Arundhati Dev Borman, Eva Lenassi, Naushin Waseem, Bev Scott, Genevieve Wright, Sophie Devery, and Ravinder Chana (UCL Institute of Ophthalmology, London, United Kingdom), and Yozo Miyake (Aichi Medical University, Aichi, Japan), for their contribution to this study.

Supported by grants from the National Institute for Health Research Biomedical Research Center at Moorfields Eye Hospital National Health Service Foundation Trust and UCL Institute of Ophthalmology (United Kingdom), Fight For Sight (United Kingdom), Moorfields Eye Hospital Special Trustees (United Kingdom), Macular Disease Society (United Kingdom), the Foundation Fighting Blindness (United States), Suzuken Memorial Foundation (Japan), Mitsukoshi Health and Welfare Foundation (Japan), and Daiwa Anglo-Japanese Foundation (Japan), and by an FFB Career Development Award (MM). The authors alone are responsible for the content and writing of the paper.

Disclosure: **K. Fujinami**, None; **N. Lois**, None; **R. Mukherjee**, None; **V.A. McBain**, None; **K. Tsunoda**, None; **K. Tsubota**, None; **E.M. Stone**, None; **F.W. Fitzke**, None; **C. Bunce**, None; **A.T. Moore**, None; **A.R. Webster**, None; **M. Michaelides**, None

References

1. Michaelides M, Hunt DM, Moore AT. The genetics of inherited macular dystrophies. *J Med Genet*. 2003;40:641–650.
2. Michaelides M, Chen LL, Brantley MA Jr, et al. ABCA4 mutations and discordant ABCA4 alleles in patients and siblings with bull's-eye maculopathy. *Br J Ophthalmol*. 2007; 91:1650–1655.
3. Lois N, Holder GE, Fitzke FW, Plant C, Bird AC. Intrafamilial variation of phenotype in Stargardt macular dystrophy—fundus flavimaculatus. *Invest Ophthalmol Vis Sci*. 1999;40: 2668–2675.
4. Lois N, Holder GE, Bunce C, Fitzke FW, Bird AC. Phenotypic subtypes of Stargardt macular dystrophy—fundus flavimaculatus. *Arch Ophthalmol*. 2001;119:359–369.
5. Lois N, Halfyard AS, Bird AC, Holder GE, Fitzke FW. Fundus autofluorescence in Stargardt macular dystrophy—fundus flavimaculatus. *Am J Ophthalmol*. 2004;138:55–63.
6. McBain VA, Townend J, Lois N. Progression of retinal pigment epithelial atrophy in Stargardt disease. *Am J Ophthalmol*. 2012;154:146–154.
7. Aaberg TM. Stargardt's disease and fundus flavimaculatus: evaluation of morphologic progression and intrafamilial coexistence. *Trans Am Ophthalmol Soc*. 1986;84:453–487.
8. Armstrong JD, Meyer D, Xu S, Elfervig JL. Long-term follow-up of Stargardt's disease and fundus flavimaculatus. *Ophthalmology*. 1998;105:448–457, discussion 457–448.
9. Fujinami K, Lois N, Davidson AE, et al. A longitudinal study of Stargardt disease: clinical and electrophysiologic assessment, progression, and genotype correlations. *Am J Ophthalmol*. 2013;155:1075–1088.
10. Fujinami K, Sergouniotis PI, Davidson AE, et al. The clinical effect of homozygous ABCA4 alleles in 18 patients. *Ophthalmology*. 2013;120:2324–2331.
11. Fujinami K, Akahori M, Fukui M, Tsunoda K, Iwata T, Miyake Y. Stargardt disease with preserved central vision: identification of a putative novel mutation in ATP-binding cassette transporter gene. *Acta Ophthalmol*. 2011;89:e297–e298.
12. Fujinami K, Sergouniotis PI, Davidson AE, et al. Clinical and molecular analysis of Stargardt disease with preserved foveal structure and function. *Am J Ophthalmol*. 2013;156:487–501.
13. Allikmets R, Shroyer NF, Singh N, et al. Mutation of the Stargardt disease gene (ABCR) in age-related macular degeneration. *Science*. 1997;277:1805–1807.
14. Allikmets R, Singh N, Sun H, et al. A photoreceptor cell-specific ATP-binding transporter gene (ABCR) is mutated in recessive Stargardt macular dystrophy. *Nat Genet*. 1997;15: 236–246.
15. Cremers FP, van de Pol DJ, van Driel M, et al. Autosomal recessive retinitis pigmentosa and cone-rod dystrophy caused by splice site mutations in the Stargardt's disease gene ABCR. *Hum Mol Genet*. 1998;7:355–362.
16. Martinez-Mir A, Paloma E, Allikmets R, et al. Retinitis pigmentosa caused by a homozygous mutation in the Stargardt disease gene ABCR. *Nat Genet*. 1998;18:11–12.
17. Fishman GA, Stone EM, Eliason DA, Taylor CM, Lindeman M, Derlacki DJ. ABCA4 gene sequence variations in patients with autosomal recessive cone-rod dystrophy. *Arch Ophthalmol*. 2003;121:851–855.
18. Sun H, Nathans J. Stargardt's ABCR is localized to the disc membrane of retinal rod outer segments. *Nat Genet*. 1997;17: 15–16.
19. Weng J, Mata NL, Azarian SM, Tzekov RT, Birch DG, Travis GH. Insights into the function of Rim protein in photoreceptors and etiology of Stargardt's disease from the phenotype in abcr knockout mice. *Cell*. 1999;98:13–23.
20. Molday LL, Rabin AR, Molday RS. ABCR expression in foveal cone photoreceptors and its role in Stargardt macular dystrophy. *Nat Genet*. 2000;25:257–258.
21. Maeda A, Maeda T, Golczak M, Palczewski K. Retinopathy in mice induced by disrupted all-trans-retinal clearance. *J Biol Chem*. 2008;283:26684–26693.

TABLE 4. Association Between AF Subtype and Genotype in 26 Patients With Two or More Disease-Causing *ABCA4* Variants

	Patients Harboring at Least One Null Variant, $n = 14$		Patients Harboring Two or More Missense Variants, $n = 12$	
	BL	FU	BL	FU
AF type 1	3 (2)	1	5 (2)	3
AF type 2	8 (2)	8	7 (1)	8
AF type 3	3	5	0	1
Total, $n = 26$	14	14	12	12

One patient harboring null variants was excluded from this analysis due to an asymmetric AF subtype at baseline (patient 61). The number of patients who showed AF subtype transition is shown in parentheses.

disease, baseline logMAR visual acuity, and logMAR visual acuity reduction. Patients with type 1 AF at baseline had a later onset of central visual loss and better visual acuity, compared to patients with type 3 AF at baseline. Correlation between duration of disease and size of atrophy, and duration of disease and RAE also were established; thereby supporting the recent suggestion that a longer disease duration is associated with more extensive and more rapidly progressive central retinal atrophy.[30]

Overall, the findings of this study suggested that patients with Stargardt disease showing localized foveal atrophy have milder progression of central atrophy compared to subjects with multiple atrophic lesions who have more rapid loss of central retinal structure over time. In contrast, patients in the "intermediate" group, with macular atrophy and a heterogeneous background, have a more variable area of atrophy and atrophy enlargement. An association between the pattern of functional loss detected on electrophysiology and the RAE was suggested in previous reports[6,30]; therefore, electrophysiological assessment may assist in the characterization of patients with an "intermediate" phenotype. Furthermore a comprehensive study of the relationship over a long-term follow-up period between AF and electrophysiology in a larger cohort of patients with Stargardt disease would be valuable.

We identified 45 likely disease-causing *ABCA4* variants, with two putative novel mutations detected. A total of 26 patients harbored two or more likely disease-causing variants; there was a statistically significant association between AF subtype classification and genotype group classification at baseline and follow-up. A difference was suggested between genotype groups in terms of proportion of AF subtypes 1 and 3, in keeping with more deleterious genetic variants being associated with a more severe and progressive AF phenotype. Sodi et al.,[54] in an AF study of 20 patients, also concluded that the presence of two severe mutations was associated with a larger area of macular atrophy.

Consistent with previous reports, four of nine patients with the c.5461-10 T>C variant had a severe phenotype, with multiple large areas of atrophy.[9,33,55,56] In contrast, there were three patients with the c.5461-10 T>C variant with a lower atrophy enlargement, all of whom also harbored missense variants (p.Gly1961Glu in one patient, and p.Leu2027Phe in the remaining two subjects); considered to be associated with a milder phenotype.[2,10,54,56,57] The substitutions p.Leu2027Phe, and to a greater extent p.Gly1961Glu, also were associated with a milder AF phenotype in our study. Larger numbers of patients are needed to investigate the phenotypic characteristics of other rare alleles.

There are several potential limitations of this study, many of which are inherent to retrospective studies, including study population selection, the variable number and interval of examinations during follow-up, the definition of atrophic lesions on AF images, AF subtype classification, and the strategy of mutation screening and genotype grouping. Of the recruited patients, 62% at baseline and 54% at follow-up were in AF subtype 2, with the number of patients with AF subtype 3 being relatively small; a larger prospective cohort will be helpful to gain an improved understanding of the pathophysiological features associated with AF subtype 3 and also address many of the aforementioned limitations of retrospective studies.

This study was designed to observe the progression between the two time points (baseline and follow-up) and the assumption of linear progression was made for atrophy enlargement in keeping with previous reports.[6,30] This study has not examined the linearity of change between baseline and follow-up testing; a prospective study with additional more frequent time point sampling will help address this pertinent question. It is possible that progression will be linear in some individuals and nonlinear in others, in keeping with the commonplace phenotypic heterogeneity of inherited retinal disorders.

The definition of the significant low gray scale on AF images can be challenging—nevertheless it is very reassuring that the two investigators in this study showed statistically significant

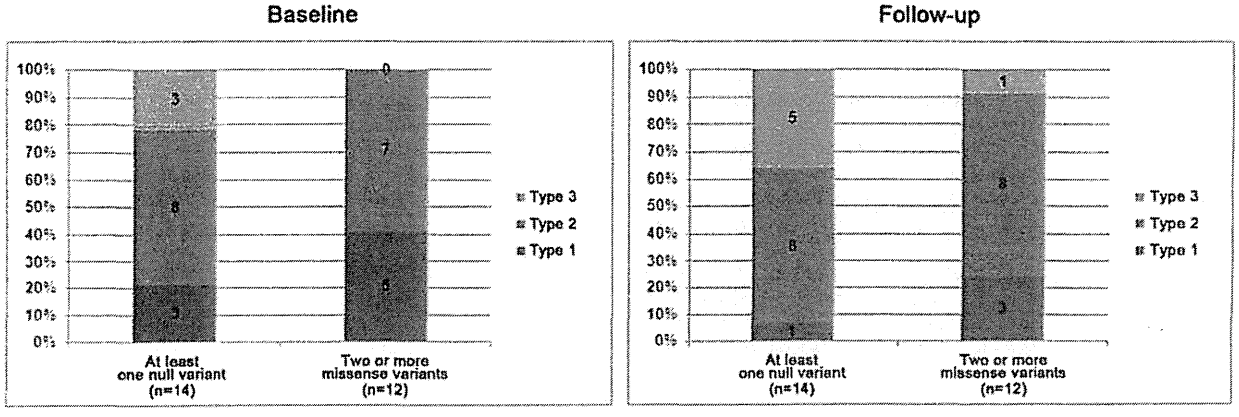

FIGURE 5. The association between genotype group and AF type at baseline and follow-up. The proportion of each AF subtype for each genotype group is shown in the *bar graphs*. In 26 patients with two or more likely disease-causing variants, there was a statistically significant association between AF subtype classification and genotype group classification at baseline and follow-up.

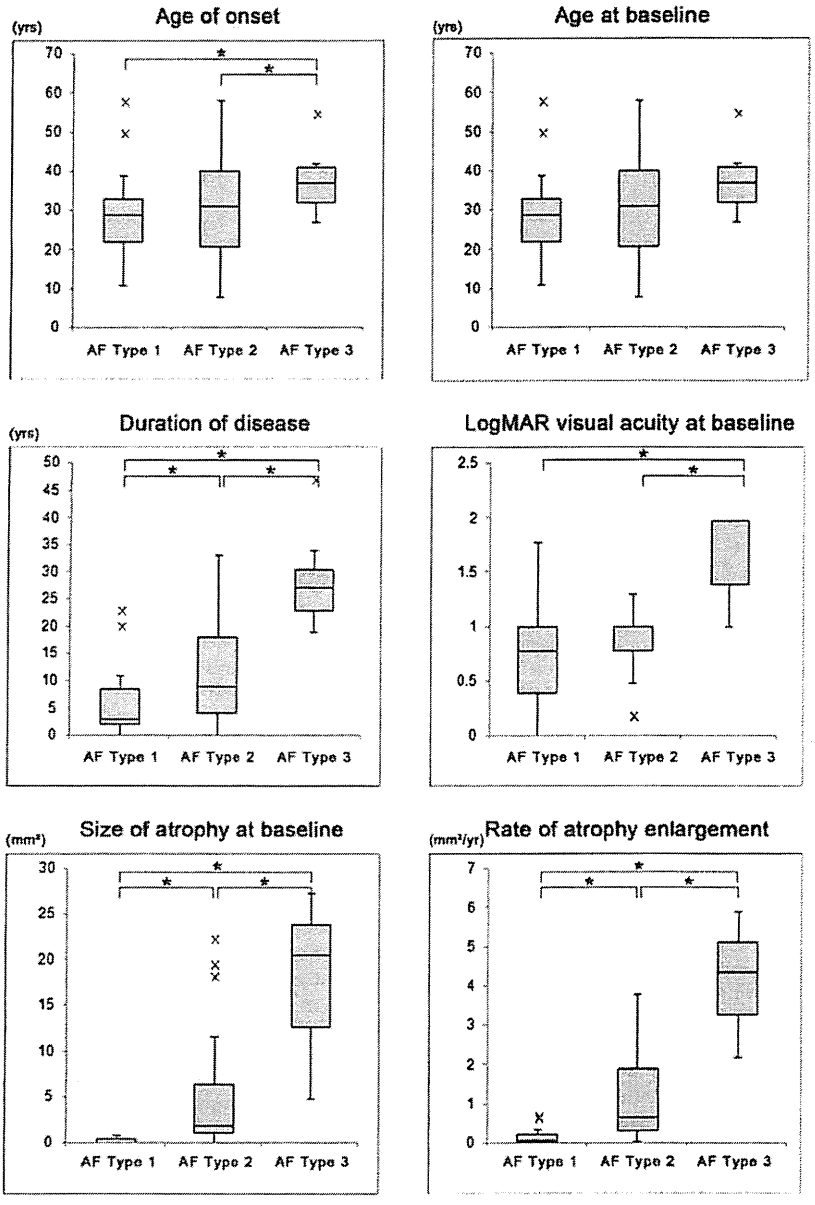

FIGURE 4. A comparison of selected clinical features and quantitative AF imaging data associated with each AF subtype at baseline in 67 patients with Stargardt disease, showing significant differences in age of onset, duration of disease, visual acuity at baseline, size of atrophy at baseline, and rate of atrophy enlargement. The *boxes* show the median, and 25% and 75% confidence interval (lower and upper quartiles). The *whiskers* extend to what could be considered the 95% confidence interval. *Crosses* represent values outside the 95% confidence interval. *Statistically significant differences.

may inform patient selection for future therapeutic interventions for *ABCA4*-related retinopathy.

We classified patients into three AF subtypes at baseline. Of patients with type 1 AF at baseline, 58% remained in type 1 AF at follow-up, whereas 12% of patients with type 2 AF showed transition to type 3 AF. Type 3 appears to be a comparatively distinct phenotype, given the fact that only a relatively small number of subjects had progression from AF type 2 to type 3, and none of the type 1 AF patients showed transition to type 3 AF. Statistically significant differences between baseline AF types in RAE also were demonstrated, suggesting a less severe and more slowly progressive phenotype in type 1 AF, and more severe and more rapid enlargement of atrophy in type 3 AF. The correlation between the total size of atrophy and RAE also supports this proposal.

There was one patient (patient 61) with an asymmetric AF subtype at baseline, type 3 in the right eye and type 2 in the left, with type 3 in both eyes at follow-up. Many possible factors may have a role in interocular asymmetry, including anisometropia, skewed X-inactivation of a modifier (in females), differences in mitochondrial sequences, somatic mutation, epigenetic differences, and "stochastic" factors (e.g., small initial differences in gene expression leading to significant differences later).

The clinical characteristics of each AF subtype showed significant differences in terms of age of onset, duration of

TABLE 3. Clinical Features and Quantitative AF Data Associated With AF Subtype at Baseline in 67 Patients With Stargardt Disease

	Median Age of Onset, y	Median Duration, y	Median Age, y		Mean Interval, y	LogMAR Visual Acuity			Median Size of Atrophy, mm²		Rate of Atrophy Enlargement, mm²/y
			BL	FU		BL	FU	Reduction	BL	FU	
Type 1, $n = 19$	24.0	3.0	29.0	36.0	9.2	0.78	1.00	0.22	0.00	1.00	0.06
Type 2, $n = 41$	18.0	9.0	31.0	38.0	9.0	1.00	1.00	0.22	1.91	8.52	0.67
Type 3, $n = 7$	8.0	27.0	37.0	43.0	9.1	1.98	1.78	0.00	20.54	57.17	4.37
Total, $n = 67$	19.0	9.0	31.0	39.0	9.1	1.00	1.00	0.12	1.12	5.32	0.45

One patient was excluded from baseline AF subtype analysis due to an asymmetric AF subtype at baseline (patient 61). The age of onset was defined as the age at which visual loss was first noted by the patient. The duration of disease was calculated as the difference between age at onset and age at the baseline examination when AF imaging was obtained. The interval of observation was determined by the difference between the age at baseline and the age at the most recent "follow-up" examination at which AF imaging was obtained. The rate of atrophy enlargement (mm²/y) was calculated as follows: size of the area of atrophy at last follow-up minus size of the area of atrophy at baseline (mm²) divided by the follow-up time (years). BL, baseline; FU, follow-up.

atrophy and median RAE associated with each baseline AF subtype are shown in Table 3 and Figure 4. There was a statistically significant difference between AF type 1 and 3, and type 2 and 3 in terms of age of onset ($P = 0.003$ and 0.016, respectively). In respect to duration of disease, there were statistically significant differences between AF types 1 and 2, types 1 and 3, and types 2 and 3 ($P = 0.018$, 0.002, and 0.001, respectively). There also was a statistically significant difference in logMAR visual acuity at baseline between AF types 1 and 3, and types 2 and 3 ($P = 0.003$ and 0.003, respectively), and in logMAR visual acuity reduction between types 1 and 3, and types 2 and 3 ($P = 0.042$ and 0.008, respectively). With respect to size of atrophy at baseline and RAE, statistically significant differences were seen between types 1 and 2, types 1 and 3, and types 2 and 3 ($P = 0.000$, $P = 0.049$, $P = 0.000$ for size of atrophy at baseline, and $P = 0.000$, $P = 0.019$, 0.014 for RAE, respectively). However, there were no statistically significant differences between AF subtypes in terms of other parameters, including age at baseline and follow-up interval.

The Spearman rank correlation test was applied for assessment of the relationships between parameters, including age of onset and size of atrophy at baseline, age at baseline and size of atrophy at baseline, duration of disease and size of atrophy at baseline, age of onset and RAE, age at baseline and RAE, duration of disease and RAE, and size of atrophy at baseline and RAE. There was a statistically significant correlation between age at baseline and size of atrophy at baseline ($\rho = 0.402$, $P < 0.0015$), duration of disease and size of atrophy at baseline ($\rho = 0.626$, $P < 0.0001$), age at baseline and RAE ($\rho = 0.369$, $P < 0.0037$), duration of disease and RAE ($\rho = 0.607$, $P < 0.0001$), and size of atrophy at baseline and RAE ($\rho = 0.767$, $P < 0.0001$). A tendency of negative correlation also was suggested between age of onset and RAE ($\rho = -0.191$, $P = 0.133$).

Molecular Genetics

Likely disease-causing variants in *ABCA4* were detected in 57 of 68 patients; with two or more variants identified in 27 patients and one variant in 30 subjects (Supplementary Table S1). Detailed results including in silico analysis are shown in Supplementary Table S2. A total of 45 variants was found in 57 patients; 13 null mutations, including one disease-associated intronic change and one predicted to affect splicing; and 32 missense variants. A total of 22 patients harbored at least one null variant, with a single subject having two null mutations. Of these 45 variants 43 have been reported previously and 2 are putative novel mutations: c.93G>A, p.Tyr31* and c.617_618delCG, p.Ser206Argfs*320 (Supplementary Tables S1, S2). The 26 patients harboring two or more disease-causing variants were classified into two genotype groups (Table 4); there were 14 patients with at least one null variant and 12 with two or more missense variants.

Genotype–AF Phenotype Correlations

The association between AF subtype and genotype group is shown in Table 4 and Figure 5. In 26 patients with two or more likely disease-causing variants, there was a statistically significant association between AF subtype classification and genotype group classification at baseline and follow-up ($\gamma = -0.567$ and $\gamma = -0.646$, respectively). There was a suggestion of a difference between the two genotype groups, in terms of proportion of AF subtypes 1 and 3. The proportion of AF subtype 1 was 21% at baseline and 7% at follow-up for the null variant genotype group, compared to 36% at baseline and 25% at follow-up for the missense variant genotype group. The proportion of AF subtype 3 was 21% and 36% at baseline and follow-up for the null variant genotype group, compared to 0% and 8% at baseline and follow-up, respectively, for the missense variant genotype group.

Four of nine patients from eight families harboring the variant c.5461-10 T>C were classified into type 3 AF at baseline and three (including one sibling pair) of these subjects had atrophy that extended beyond the limits of the AF image obtained (Supplementary Table S1). The median size of atrophy at baseline and follow-up in the remaining six patients was 0.92 and 6.29 mm², respectively. The median RAE of these patients harboring the variant c.5461-10 T>C was 0.45 mm²/y.

Four of eight patients from eight families harboring the missense variant p.Leu2027Phe had small central atrophy (<0.18 mm²) at baseline (Supplementary Table S1). The median size of atrophy at baseline and median RAE of these eight patients was 0.27 mm² and 0.39 mm²/y. respectively, which are less than the median values for the entire cohort of 68 patients (1.12 mm² and 0.45 mm²/y). The median size of atrophy at baseline and the median RAE of the five patients from five families harboring the missense variant p.Gly1961Glu also was relatively small; 0.47 mm² and 0.20 mm²/y respectively (Supplementary Table S1).

DISCUSSION

This study assessed longitudinal changes in RPE atrophy by undertaking AF imaging in a large well-characterized cohort of patients with Stargardt disease; 84% of subjects harbored at least one likely disease-causing *ABCA4* allele. The findings herein assist in providing improved advice on prognosis and

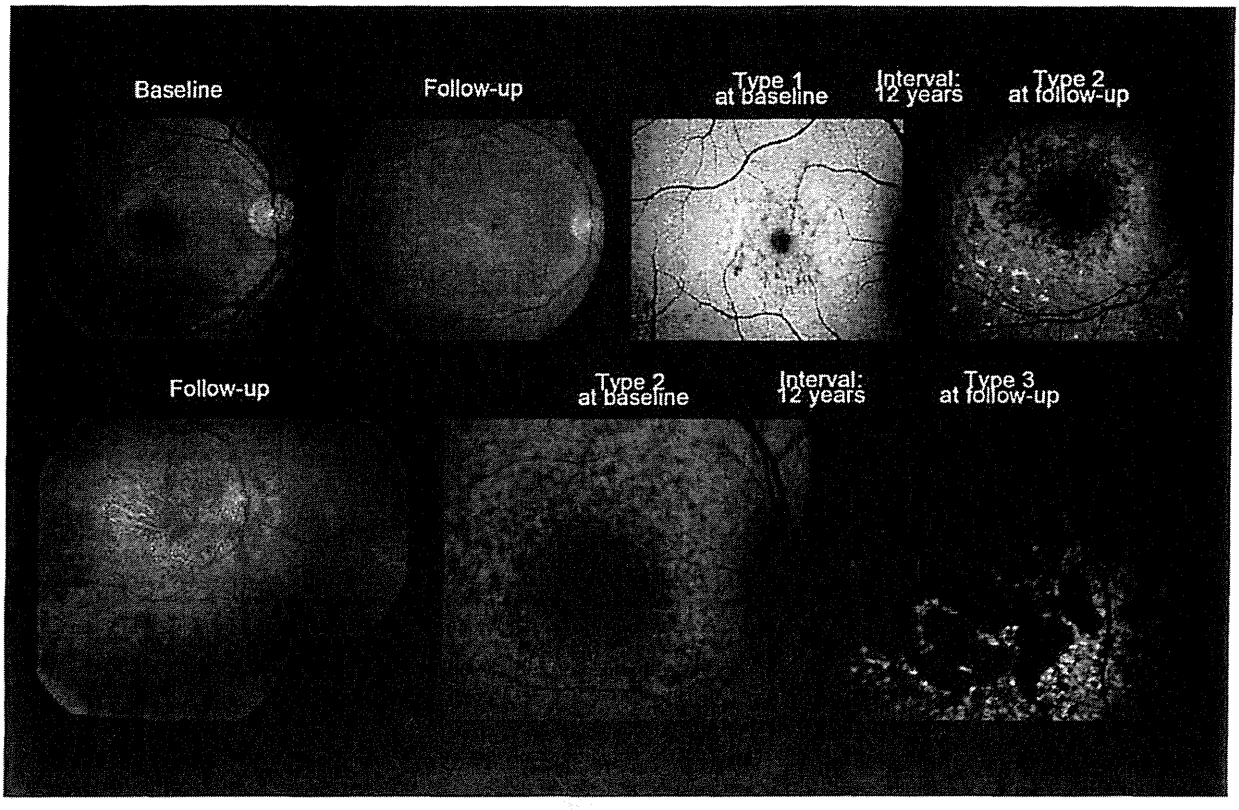

FIGURE 3. Color fundus photographs and AF images of two representative cases with Stargardt disease, showing AF subtype transition over time (patients 12 and 59). *Top row*: Color fundus photographs of patient 12 showing mild foveal atrophy surrounded by parafoveal yellowish-white flecks at baseline and more marked macular atrophy surrounded by numerous atrophic flecks extending anterior to the vascular arcades at follow-up. AF imaging demonstrates localized low signal at the fovea surrounded by a homogeneous background with high and low signal parafoveal foci at baseline, and a macular low signal lesion surrounded by numerous high and low signal foci throughout the posterior pole with a heterogeneous background at follow-up, consistent with transition from AF type 1 to type 2. *Bottom row*: Patient 59 had extensive areas of atrophy extending beyond the vascular arcades with atrophic flecks at follow-up. AF imaging showed subtype transition; a mottled macular low signal lesion surrounded by numerous low signal foci with a heterogeneous background (type 2) at baseline, and multiple areas of low signal throughout the posterior pole with a heterogeneous background (type 3) at follow-up. The central atrophy at follow-up extended beyond the limits of the AF image ("beyond the scope").

(patients 11, 31, 36, 39, 44, 56) had unavailable AF images at baseline of the left eye.

At baseline, 67 patients were classified based on the AF findings into three subtypes: 19 patients (28%) in type 1, 41 (61%) in type 2, and 7 (10%) in type 3. At follow-up there were 11 (16%) in type 1, 44 (66%) in type 2, and 12 (18%) in type 3 (Table 2). All patients had a symmetrical AF subtype between eyes, except for patient 61 with type 3 in the right and type 2 in the left at baseline, with type 3 chosen as the overall classification for this patient.

A total of 13 patients (28%) showed AF subtype transition during follow-up; 8/19 (42%) subjects from AF type 1 to AF type 2, and 5/41 (12%) individuals from AF type 2 to AF type 3 (Table 2). Three of five sibships were concordant for AF subtype at baseline (patients 31 and 37; 35 and 36; and 63 and 64) and two of five were discordant (patients 13 and 23; and 18 and 23); all the sibships were concordant at follow-up (Supplementary Table S1).

A total of 13 patients (19%) at baseline and 2 (2%) at follow-up had a single small area of low signal (<0.18 mm^2) in the selected eye and were recorded as having zero mm^2 of atrophy (Supplementary Table S1). There were six patients who had atrophy in the selected eye extending beyond the limits of the AF image at baseline and, thereby, they were excluded from the quantitative analyses (Supplementary Table S1). The median total size of atrophy at baseline and follow-up was 1.12 mm^2 (range, 0.00–27.23) and 5.32 mm^2 (range, 0.00–62.58), respectively. The median RAE over time was 0.45 mm^2/y (range, 0.00–5.89). The concordance correlation coefficient revealed significant agreement between the two observers' measurements (concordance correlation coefficient was 0.99). The clinical features of each baseline AF subtype are summarized in Table 3 and Figure 4. The median size of

TABLE 2. Distribution and Transition of AF Subtypes of 67 Patients With Stargardt Disease

	AF Type at Follow-up		
	Type 1	Type 2	Type 3
AF type at baseline			
Type 1, $n = 19$	11	8	0
Type 2, $n = 41$		36	5
Type 3, $n = 7$			7
Total, $n = 67$	11	44	12

One patient was excluded for this analysis due to an asymmetric AF subtype at baseline (patient 61).

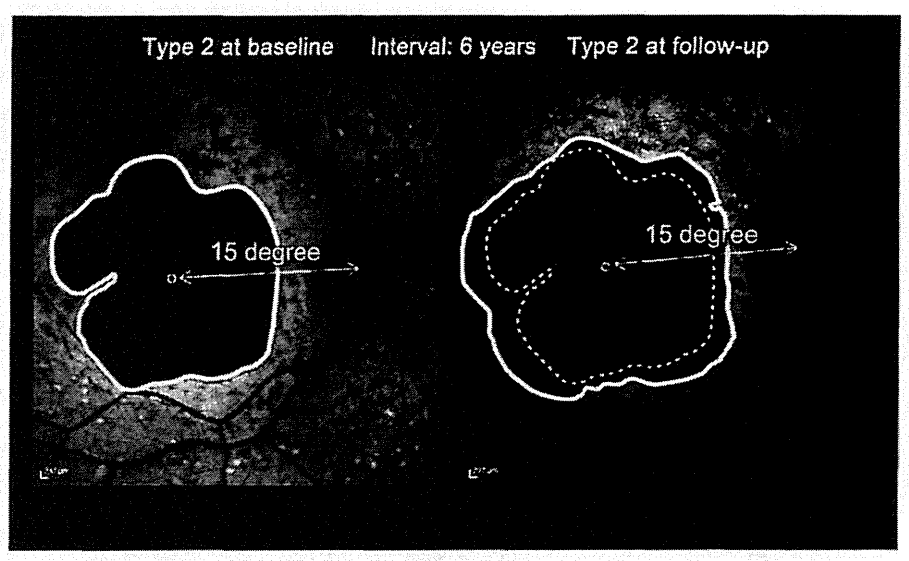

FIGURE 2. Measurement of the low signal area of AF and calculation of the rate of atrophy enlargement in a representative case with Stargardt disease. The area of low AF signal (patient 51) was measured using custom software, which enables measurement of the dimensions of the area outlined manually (*white line* in the *left* and *right* images) and the automatic computation of the area expressed in square degrees to facilitate the appreciation of the relation to the patient's visual function; with a given distance between the center of the optic nerve head and the foveola defined as 15° (marked in the images). Atrophy enlargement over time was calculated as the difference between the size of atrophy at baseline and follow-up (*broken white line* and *continuous white line* of the *right* image). The rate of atrophy enlargement (mm^2/y) was obtained as the atrophy enlargement (mm^2) divided by the follow-up time (years).

Mutation Screening

Mutation screening was performed using the single-stranded conformation polymorphism (SSCP) strategy in 35 subjects,[50] and the arrayed primer extension (APEX) microarray (ABCR400 chip; Asper Ophthalmics, Tartu, Estonia) in 33 patients.[51] All the variants detected were confirmed with direct Sanger sequencing. Direct Sanger sequencing also was performed in siblings of probands and parents when available to confirm segregation of alleles.

Nonnull variants were analyzed using two software prediction programs: Sorting Intolerant from Tolerance (SIFT, available in the public domain at http://sift.jcvi.org/),[52] and PolyPhen2 (available in the public domain at http://genetics.bwh.harvard.edu/pph/index.html).[53] All variants were compared to variants in the Exome Variant Server; National Heart, Lung, and Blood Institute (NHLBI) Exome Sequencing Project, Seattle, Washington (available in the public domain at http://snp.gs.washington.edu/EVS/).

Patients harboring two or more mutations were classified into two mutually exclusive genotype groups on the basis of the molecular analysis: patients with at least one null variant, (group A) and subjects with two or more missense variants (group B). Only patients harboring two or more likely disease-causing variants were included to investigate genotype-phenotype correlations. Null variants were those that would be expected to affect splicing, or to introduce a premature truncating codon in the protein if translated. One disease-associated intronic change with uncertain effect was treated as a null allele due to the associated severe clinical phenotype previously reported.[9,33]

Statistical Analysis

Statistical methods are provided in Supplementary Material S1.

RESULTS

Clinical Findings

We included in the study 68 patients with a clinical diagnosis of Stargardt disease. The clinical findings are summarized in Supplementary Table S1. There were 36 female (53%) and 32 male patients (47%). All complained of central visual loss, with a median age of onset of 19.0 years (range, 5–48 years) and a median duration of disease of 9.0 years (range, 0–47 years). One patient had relative foveal sparing in the left eye on AF imaging at presentation (patient 24; age of onset, 48 years). The median ages at baseline and at follow-up were 30.5 and 39.0 years (range, 8–58 and 18–67), respectively. The mean follow-up interval was 9.1 years (range, 6–13). Seven patients (10%) presented before 16 years of age and 61 patients (90%) presented after 16 years. The median logMAR visual acuities at baseline and at follow-up were 1.00 (range, 0.0–1.98) and 1.00 (0.0–2.28), respectively, with a median logMAR visual acuity reduction during the follow-up interval of 0.15 (range, –0.78–1.28).

Color fundus photographs and AF images of representative cases are shown in Figures 1 and 3; with three representative cases without AF type transition during follow-up in Figure 1, and two cases with AF type transition in Figure 3.

Fundus AF Findings

The AF imaging at baseline was obtained with the Zeiss system in 52 patients and with the HRA2 in 16 subjects. The AF imaging at follow-up was obtained with the HRA2 or Spectralis (field of view 30° × 30°) in all 68 individuals, with additional wide-field images (55° × 55°) undertaken in 19 patients. Complete AF data sets were available at baseline and follow-up with few exceptions; in patient 28, AF images were unavailable of the right eye at baseline and follow-up, and six patients

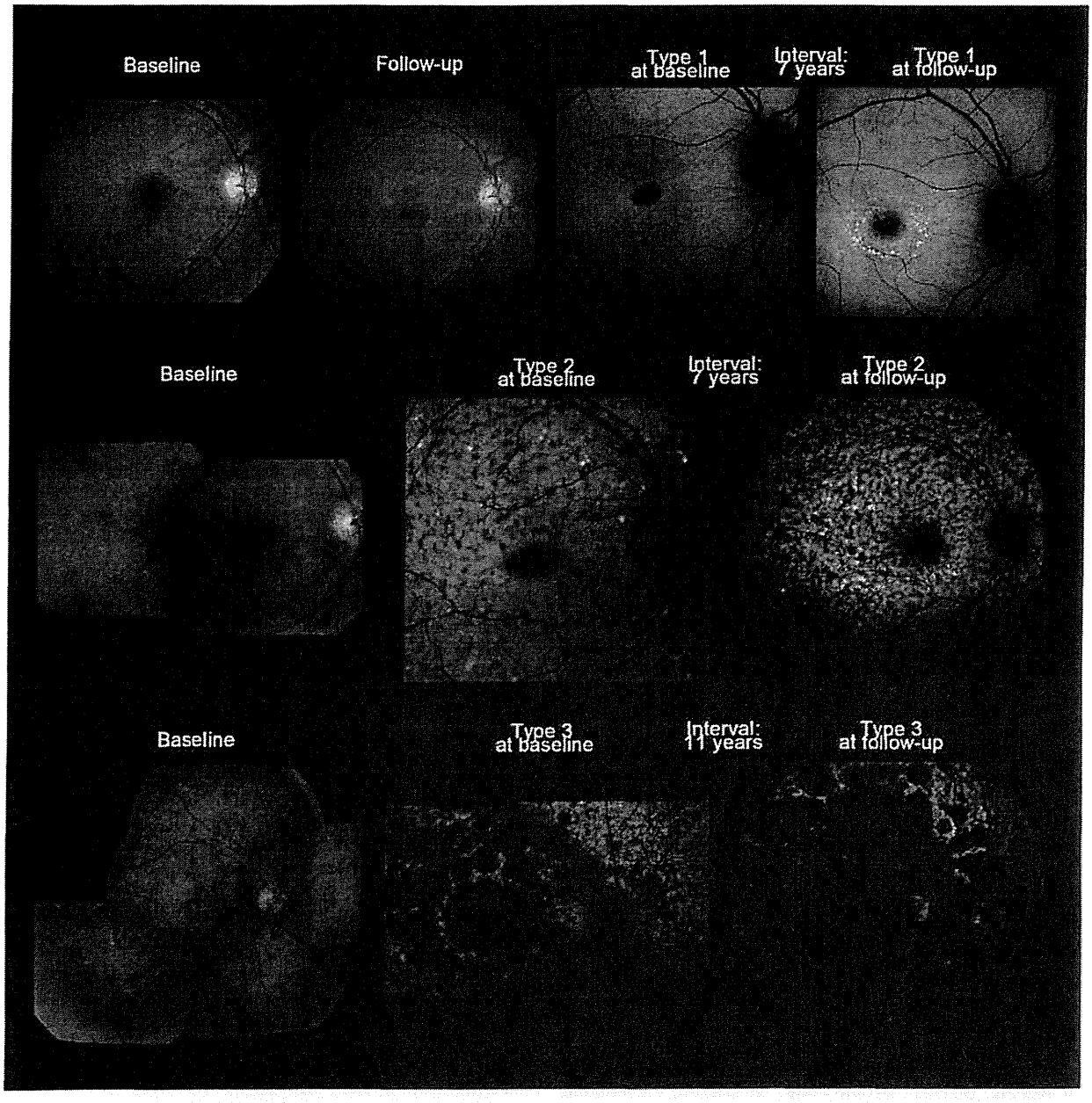

FIGURE 1. Color fundus photographs and AF images of three representative cases with Stargardt disease, illustrating the three AF subtypes in subjects where there was no subtype transition over time (patients 7, 50, and 54). *Top row*: Color fundus photographs of patient 7 showing subtle RPE changes at the fovea at baseline with a mild increase in the degree of atrophy at follow-up. AF imaging demonstrates a localized low signal lesion with a relatively high signal edge and a homogeneous background at baseline, and a low signal foveal lesion surrounded by patchy small foci with high signal and a homogeneous background at follow-up; consistent with AF type 1 at baseline and follow-up. *Middle row*: Patient 50 had macular atrophy surrounded by yellowish-white flecks extending anterior to the vascular arcades at baseline, and a low signal area at the macula surrounded by high and low foci throughout the posterior pole (AF type 2) at baseline and follow-up, with a heterogeneous background at baseline and follow-up. *Bottom row*: Patient 65 had extensive areas of atrophy throughout the posterior pole, extending beyond the vascular arcades, with yellowish-white and atrophic flecks at baseline, and multiple areas of low signal with heterogeneous background (AF type 3) at baseline and follow-up.

Where possible, AF images with a 30° × 30° field were used for RAE analysis ($n = 68$ at baseline and $n = 67$ at follow-up). For patients with AF images available in both eyes at baseline and follow-up ($n = 61$), the eye used for analysis was selected according to the Random Integer Generator (available in the public domain at http://www.random.org/), and for individuals with AF imaging available in only one eye ($n = 7$), that eye was selected for analysis. Patients who had central atrophy that extended beyond the limits of the AF images obtained with field of view 30° × 30° were excluded from the size of atrophy and RAE analyses ($n = 6$).

TABLE 1. Definition of Fundus AF Subtypes in Stargardt Disease

Type 1	Localized low AF signal at the fovea surrounded by a homogeneous background with/without perifoveal foci of high or low signal
Type 2	Localized low AF signal at the macula surrounded by a heterogeneous background and widespread foci of high or low AF signal extending anterior to the vascular arcades
Type 3	Multiple areas of low AF signal at posterior pole with a heterogeneous background with/without foci of high or low signal

It has been challenging in Stargardt disease to establish comprehensive genotype-phenotype correlations due to the variable phenotype and the heterogeneity of *ABCA4*; more than 700 sequence variants have been reported.[1,2,9-15,31-44] A previous cross-sectional study of 43 patients with Stargardt disease demonstrated that AF patterns appeared to relate to functional abnormalities.[5] A recent small AF study ($n = 12$) demonstrated variable rates of enlargement of RPE atrophy in Stargardt disease, with a strong association between atrophy enlargement and electrophysiological grouping.[6] Chen et al.[30] also have reported the progressive change in the area of atrophy in 52 patients with Stargardt disease over a mean follow-up of 2.92 years; with variable atrophy progression demonstrated, and an association with electrophysiological findings. However, comprehensive investigations over a long-term follow-up of a large cohort of patients with Stargardt disease, including AF imaging, clinical assessment, and molecular analysis still are lacking.

The purpose of this study was to characterize the subtypes of AF and investigate the enlargement of RPE atrophy in patients with Stargardt disease in a longitudinal survey with a mean follow-up of 9 years. This study also provided an opportunity to investigate the association of these AF subtypes and atrophy progression with the detailed clinical and molecular genetic findings.

METHODS

Patients

A cohort of 68 patients with a clinical diagnosis of Stargardt disease and a minimum of 6 years of follow-up were ascertained at Moorfields Eye Hospital.

For the purpose of this study, patients with a clinical history compatible with Stargardt disease and clinical signs of bilateral macular atrophy, with or without surrounding flecks, were included. The clinical features of 42 patients in this cohort have been described partially in an earlier report, which did not include AF findings.[9] The panel included five sibling pairs. After informed consent was obtained, blood samples were taken for DNA extraction and mutation screening of *ABCA4*. The protocol of the study adhered to the provisions of the Declaration of Helsinki and was approved by the local Ethics Committee of Moorfields Eye Hospital.

Clinical Assessment

We assessed 68 patients on at least two occasions, with the first and most recent visits taken as the baseline and "follow-up" examinations, respectively, for the purposes of data analysis. A full medical history was obtained and a comprehensive ophthalmologic examination performed. The age of onset was defined as the age at which visual loss was first noted by the patient. The duration of the disease was calculated as the difference between age at onset and age at the baseline examination when AF imaging was obtained. The interval of observation was determined by the difference between the age at baseline and the age at the most recent "follow-up" examination when AF imaging was done.

Best-corrected Snellen visual acuity was converted to equivalent logMAR visual acuity,[45] and visual acuity reduction was calculated as the difference between logMAR visual acuity at baseline and follow-up.

Fundus AF Imaging

The AF imaging was performed using a confocal scanning laser ophthalmoscope (cSLO). Baseline images were obtained before 2003 using a Zeiss prototype cSLO (SM 30-4024, excitation light 488 nm, barrier filter 521 nm, field of view 30° × 30°; Carl Zeiss Meditec, Oberkochen, Germany).[5,29,46-48] From 2003 to 2009, images were obtained using an HRA2 (excitation light 488 nm, barrier filter 500 nm, field of view 30° × 30°; Heidelberg Engineering GmbH, Heidelberg, Germany).[47] After 2009, images were obtained using the Spectralis with viewing module version 5.1.2.0 (excitation light 488 nm, barrier filter 500 nm, fields of view 30° × 30° and 55° × 55°; Heidelberg Engineering GmbH).[49]

Patients were classified into 3 AF subtypes based on a recent report of AF findings in Stargardt disease:[10] type 1 - localized low AF signal at the fovea surrounded by a homogeneous background, with/without perifoveal foci of high or low AF signal; type 2 - localized low AF signal at the macula surrounded by a heterogeneous background, and widespread foci of high or low AF signal extending anterior to the vascular arcades; and type 3 - multiple areas of low AF signal at the posterior pole with a heterogeneous background, with/without foci of high or low AF signal (Table 1, Fig. 1). In previously published reports, the progression of atrophy has been influenced by two patterns of background AF ("homogeneous" and "heterogeneous"),[6] and multiple atrophic lesions at the posterior pole have been associated with a more rapid functional deterioration.[9] The data of AF subtypes obtained at follow-up were compared to those at baseline. A patient (patient 61) who had an asymmetric AF subtype was excluded from the AF subtype analysis.

Areas of low AF signal were measured using custom software (Retinal analysis tool; Halfyard AS, Fitzke FW, University College London [UCL] Institute of Ophthalmology, London, UK). With reference to a given distance between the center of the optic nerve head and the foveola, which is defined as 15°, this software enables measurement of the dimensions of the area tracked manually and computation of the size expressed in square degrees automatically (Fig. 2). The significant low gray scale point on the images was decided upon by agreement between the two investigators (KF, RM) and the dimension of the area within the tracked line of low gray scale was calculated.

All the values in square degrees were converted to square millimeters using the previously reported conversion factor (1° = 0.3 mm; Fitzke FW. *IOVS* 1981;20(suppl):ARVO Abstract 144). Only low AF signal lesions of >0.18 mm^2 in size were considered. The total area of atrophy was calculated by summation of all the measured low signal lesions. All of these measurements were conducted by two investigators (KF, RM), and the averaged values were used for final analyses. The rate of atrophy enlargement (RAE, mm^2/y) was calculated as follows according to previous reports[6,30]: size of the area of atrophy at last follow-up minus size of the area of atrophy at baseline (mm^2) divided by the follow-up time (years) (Fig. 2).

A Longitudinal Study of Stargardt Disease: Quantitative Assessment of Fundus Autofluorescence, Progression, and Genotype Correlations

Kaoru Fujinami,[1-4] Noemi Lois,[5] Rajarshi Mukherjee,[1,2] Vikki A. McBain,[6] Kazushige Tsunoda,[3] Kazuo Tsubota,[4] Edwin M. Stone,[7] Fred W. Fitzke,[1] Catey Bunce,[1,2] Anthony T. Moore,[1,2] Andrew R. Webster,[1,2] and Michel Michaelides[1,2]

[1]University College London Institute of Ophthalmology, London, United Kingdom
[2]Moorfields Eye Hospital, London, United Kingdom
[3]Laboratory of Visual Physiology, National Institute of Sensory Organs, National Hospital Organization, National Tokyo Medical Center, Meguro-ku, Tokyo, Japan
[4]Department of Ophthalmology, Keio University School of Medicine, Shinjyuku-ku, Tokyo, Japan
[5]Clinical Ophthalmology at the Centre for Vision and Vascular Science, Queens University Belfast, Belfast, Northern Ireland
[6]Department of Ophthalmology, Institute of Medical Sciences, University of Aberdeen, Aberdeen, Scotland, United Kingdom
[7]University of Iowa, Institute for Vision Research, Howard Hughes Medical Institute, Iowa City, Iowa

Correspondence: Michel Michaelides, UCL Institute of Ophthalmology, 11-43 Bath Street, London EC1V 9EL, UK;
michel.michaelides@ucl.ac.uk.

Submitted: March 26, 2013
Accepted: November 8, 2013

Citation: Fujinami K, Lois N, Mukherjee R, et al. A longitudinal study of Stargardt disease: quantitative assessment of fundus autofluorescence, progression, and genotype correlations. *Invest Ophthalmol Vis Sci.* 2013;54:8181–8190. DOI:10.1167/iovs.13-12104

Purpose. We characterized subtypes of fundus autofluorescence (AF) and the progression of retinal atrophy, and correlated these findings with genotype in Stargardt disease.

Methods. Full clinical examination and AF imaging was undertaken in 68 patients with Stargardt disease. The baseline data were compared to those at follow-up. Patients were classified into three AF subtypes: type 1 had a localized low signal at the fovea surrounded by a homogeneous background, type 2 had a localized low signal at the macula surrounded by a heterogeneous background with numerous foci of abnormal signal, and type 3 had multiple low signal areas at the posterior pole with a heterogeneous background. At baseline, there were 19 patients with type 1, 41 with type 2, and 8 with type 3 disease. The areas of reduced AF signal were measured and rate of atrophy enlargement (RAE) was calculated as the difference of the atrophy size over time (mm^2) divided by the follow-up interval (years). Molecular screening of *ABCA4* was undertaken.

Results. The mean follow-up interval was 9.1 years. A total of 42% cases with type 1 disease progressed to type 2, and 12% with type 2 progressed to type 3. The RAE (mm^2/y) based upon baseline AF subtypes was significantly different; 0.06 in type 1, 0.67 in type 2, and 4.37 in type 3. *ABCA4* variants were identified in 57 patients. There was a significant association between AF subtype and genotype.

Conclusions. The AF pattern at baseline influences the enlargement of atrophy over time and has genetic correlates. These data are likely to assist in the provision of counseling on prognosis in Stargardt disease and be valuable for future clinical trials.

Keywords: Stargardt, ABCA4, autofluorescence

Stargardt disease is the most common inherited macular dystrophy, and is associated with a variable phenotype and disease severity.[1-12] Stargardt disease typically presents with central macular atrophy and yellow-white flecks at the posterior pole, primarily at the level of the RPE. Progressive retinal degeneration over time, including development/resorption of flecks, atrophy enlargement, and deterioration of retinal function, has been reported in Stargardt disease.[7-9] Mutations in the gene *ABCA4* underlie Stargardt disease, and also have been implicated in cone dystrophy, cone-rod dystrophy, and "retinitis pigmentosa."[2,9,10,13-17] The *ABCA4* gene encodes a transmembrane rim protein in the outer segment discs of photoreceptors that is involved in active transport of retinoids from photoreceptor to RPE.[18-24] Failure of this transport results in accelerated deposition of a major lipofuscin fluorophore, N-retinylidene-N-retinylethanolamine (A2E), in the RPE.[20-22] A2E and other lipofuscin fluorophores are elevated dramatically in the RPE of postmortem samples from patients with Stargardt disease and in *ABCA4* knockout mice (*abca4*$^{-/-}$).[19,25] Over time, A2E-associated cytotoxicity is believed to cause RPE dysfunction and cell death, with subsequent photoreceptor cell loss.[26,27]

Autofluorescence (AF) imaging can provide useful information about the distribution of lipofuscin in the RPE, and give indirect information on the level of metabolic activity of the RPE; lipofuscin levels are determined largely by the rate of turnover of photoreceptor outer segments.[28,29] The abnormal accumulation of lipofuscin, the presence of active and resorbed flecks, and RPE atrophy leads to a characteristic appearance on AF imaging in Stargardt disease; very low AF signals in photoreceptor and RPE atrophy, and foci with low or high AF signals due to flecks.[5,6,10,30]

Copyright 2013 The Association for Research in Vision and Ophthalmology, Inc.

SUPPLEMENTAL TABLE 7. Investigation of the Pathogenicity of Identified ABCA4 Variants (*Continued*)

Exon	Nucleotide Substitution and Amino Acid Change	Number of Alleles	Previous Report	SIFT[a] Pred.	SIFT[a] Index (0-1)	PolyPhen 2[a] Pred.	PolyPhen 2[a] Hum Var Score (0-1)	HSF Matrix[a] Site Affected	HSF Matrix[a] Wt CV	HSF Matrix[a] Mt CV	HSF Matrix[a] CV % Variation	Allelic Frequency Observed by EVS[a]	Reference
43	c.5908 C>T, p.Leu1970Phe	1	Lewis[25]	Tol.	0.14	PRD	0.997				No change	ND	
44	c.6079 C>T, p.Leu2027Phe	4	Allikmets[11]	Intol.	0.02	PRD	0.999				No change	3/10 758	db SNP (rs61751408)
44	c.6089 G>A, p.Arg2030Gln	2	Lewis[25]	Tol.	0.1	PRD	0.999				No change	6/10 758	db SNP (rs61750541)
46	c.6320 G>A, p.Arg2107His	2	Fishman[21]	Intol.	0	PRD	0.996				NA	83/10 758	db SNP (rs62642564)
47	c.6449 G>A, p.Cys2150Tyr	5	Fishman[21]	Intol.	0	PRD	0.995	Don.	76.6	49.8	Site broken (−35.02)	1/10 758	db SNP (rs61751384)

Acc. = acceptor site; Don. = donor site; EVS = Exome Variant Server; HSF = Human Splicing Finder program; Hum Var = Human Var score; Int. = intron; Intol. = intolerant; Mt CV = mutant consensus value; NA = not applicable; ND = not detected; PRD = probably damaging; Pred. = prediction; SIFT = Sorting Intolerant from Tolerance program; Tol. = tolerant; Wt CV = wild-type consensus value.

[a]SIFT (version 4.0.4) results are reported to be tolerant if tolerance index ≥ 0.05 or intolerant if tolerance index < 0.05. PolyPhen-2 (version 2.1) appraises mutations qualitatively as Benign, Possibly Damaging, or Probably Damaging based on the model's false-positive rate. The cDNA is numbered according to Ensembl transcript ID ENST00000370225, in which +1 is the A of the translation start codon. Human Splicing Finder (HSF, version 2.4.1) reports the results from the HSF matrix: the higher the consensus value (CV), the stronger the predicted splice site. The values for the wild-type and mutant sequences are shown; the larger the difference between these values, the greater the chance that the variant can affect splicing. EVS denotes variants in the Exome Variant Server, NHLBI Exome Sequencing Project, Seattle, WA, USA (accessed January 12, 2012; http://snp.gs.washington.edu/EVS/).

SUPPLEMENTAL TABLE 7. Investigation of the Pathogenicity of Identified *ABCA4* Variants

Exon	Nucleotide Substitution and Amino Acid Change	Number of Alleles	Previous Report	SIFT* Pred.	SIFT* Index (0-1)	PolyPhen 2* Pred.	PolyPhen 2* Hum Var Score (0-1)	HSF Matrix* Site Affected	HSF Matrix* Wt CV	HSF Matrix* Mt CV	HSF Matrix* CV % Variation	Allelic Frequency Observed by EVS*	Reference
3	c.161 G>A, p.Cys54Tyr	3	Lewis[25]	Tol.	0.11	PRD	0.994				No change	1/10 758	db SNP (rs150774447)
3	c.286 A>C, p.Asn96His	1	Papaioannou[26]	Tol.	0.14	PRD	0.994				No change	1/10 758	db SNP (rs61748529)
5	c. 466 A>G, p. Ile156 Val	2	Papaioannou[26]	Tol.	0.46	Benign	0.003				No change	11/10 758	db SNP (rs112467008)
6	c.768 G>T, p.Val256Val/Splice site	1	Klevering[24]	Tol.	0.56	NA		Don.	70.4	58	Site broken (−17.51)	ND	
9	c.1222 C>T, p.Arg408*	1	Webster[29]	NA		NA							
10	c.1253 T>C, p.Phe418Ser	1	Zernant[30]	Intol.	0	PRD	0.99				No change	ND	
10	c.1317 G>A, p.Trp439*	2	This study	NA		NA						ND	
12	c.1721delAC, p.Asp574Aspfs*582	1	Briggs[20]	NA		NA		Acc.	47.2	68.3	New site (44.5)	ND	
14	c.1957 C>T, p.Arg653Cys	1	Rivera[27]	Tol.	0.1	PRD	0.999				No change	1/10 758	db SNP (rs141823837)
14	c.2023 G>A, p.Val675Ile	1	This study	Tol.	0.07	PRD	0.989				NA	ND	
15	c.2239delC, p.Leu747Cysfs*787	1	This study	NA		NA		Don.	34.7	77	New site (+122)	ND	
17	c.2588 G>C, p.Gly863Ala	8	Allikmets[11]	Intol.	0.01	PRD	0.996				No change	53/10 758	db SNP (rs76157638)
19	c.2791 G>A, p.Val931Met	1	Allikmets[10]	Tol.	0.12	PRD	0.716				No change	18/10 758	db SNP (rs58331765)
19	c.2828 G>A, p.Arg943Gln	3	Webster[29]	Intol.	0.03	Benign	0.449	Acc.	52.2	81.1	New site (+55.48)	340/10 758	db SNP (rs1801581)
19	c.2894 A>G, p.Asn965Ser	1	Lewis[25]	Intol.	0	PRD	0.981	Acc.	53.4	82.3	New site (+54.26)	ND	
21	c.3056 C>T, p.Thr1019Met	2	Rozet[28]	Intol.	0	PRD	0.999				No change	ND	
22	c.3211_3212insGT, p.Ser1071Cysfs*1084	2	Allikmets[10]	NA		NA		Don.	69.3	28	Site broken (−59.55)	ND	
22	c.3259 G>A, p.Glu1087Lys	1	Lewis[25]	Intol.	0	PRD	0.997				No change	ND	
22	c.3322 C>T, p.Arg1108Cys	2	Rozet[28]	Intol.	0	PRD	0.986				No change	1/10 758	db SNP (rs61750120)
22	c.3323 G>A, p.Arg1108His	1	Webster[29]	Intol.	0	PRD	0.986				No change	ND	
28	c.4139 C>T, p.Pro1380Leu	4	Lewis[25]	Intol.	0.01	Benign	0.377				No change	2/10 758	db SNP (rs61750130)
Int. 28	c.4253+5 G>T, Splice site	1	Lewis[25]	NA		NA		Don.	87.9	75.6	Site broken (−14.02)	1/10 758	
29	c.4328 G>A, p.Arg1443His	1	Jaakson[23]	Tol.	0.19	PRD	0.996				No change	ND	
30	c. 4363 C>T, p. Cys1455Arg	1	This study	Tol.	0.34	PRD	0.994				NA	ND	
30	c.4469 G>A, p.Cys1490Tyr	1	Webster[29]	Intol.	0.03	PRD	0.994				No change	ND	
30	c.4519 G>A, p.Gly1507Arg	1	This study	Tol.	0.48	PRD	0.996	Acc.	78.9	78.9	New site (+58.11)	ND	
30	c.4537_4538insC, p.Gly1513Profs*1554	1	Briggs[20]	NA		NA		Acc.	91.7	33.3	Site broken (−63.76)	ND	
35	c.4918 C>T, p.Arg1640Trp	1	Rozet[28]	Intol.	0	PRD	1				No change	ND	
35	c.4956 T>G, p.Tyr1652*	1	Fumagalli[22]	NA		NA							
Int. 38	c.5461-10 T>C	9	Briggs[20]	NA		NA						3/10 758	db SNP (rs1800728)
39	c. 5516 T>C, p. Phe1839Ser	1	This study	Intol.	0	PRD	0.988				No change	ND	
Int. 40	c.5714+5 G>A, Splice site	1	Cremers[13]	NA		NA		Donor	85.5	73.3	Wild-type site broken (−14.23)	ND	
42	c.5882 G>A, p.Gly1961Glu	1	Allikmets[11]	Tol.	0.18	PRD	1				No change	29/10 758	db SNP (rs1800553)

Continued on next page

SUPPLEMENTAL TABLE 6. Electrophysiologic Group Transition and ABCA4 Variantsa Identified in 59 Patients With Stargardt Disease (*Continued*)

Pt	Electrophysiologic Group (BL / FU)	Genotype Group	Number of Variants	Exon	Nucleotide Substitution	Amino Acid Change	Screening Method (Yes/No)		
							SSCP	APEX	DS
35	II / II	B	2	3	c.161 G>A	p.Cys54Tyr	✓	—	—
				17	c.2588 G>C	p.Gly863Ala	✓	—	—
36	II / II	A	2	19	c.2791 G>A	p.Val931Met	—	✓	—
				Int. 38	c.5461-10 T>C	Splice site	—	✓	—
37	II / III	C	1	28	c.4139 C>T	p.Pro1380Leu	—	✓	—
38	II / III	A	2	22	c.3211_3212insGT	p.Ser1071Cysfs*1084	—	✓	—
				28	c.4139 C>T	p. Pro1380Leu	—	✓	—
39	II / III	A	2	Int. 38	c.5461-10 T>C	Splice site	—	✓	—
				Int. 40	c.5714+5 G>A	Splice site	—	✓	—
40	II / III	D	0				✓	—	—
41	II / III	D	0				✓	—	—
42	II / III	C	1	3	c.161 G>A	p.Cys54Tyr	✓	—	—
43	II / III	D	0				✓	—	—
44	II / III	C	1	19	c.2894 A>G	p.Asn965Ser	✓	—	—
45	III / III	C	1	21	c.3056 C>T	p.Thr1019Met	✓	—	—
46	III / III	C	1	21	c.3056 C>T	p.Thr1019Met	✓	—	—
47	III / III	C	1	47	c.6449 G>A	p.Cys2150Tyr	✓	—	✓
48	III / III	A	2	Int. 38	c.5461-10 T>C	Splice site	—	✓	—
				44	c.6079 C>T	p.Leu2027Phe	—	✓	—
49	III / III	A	1	12	c.1721delAC	p.Asp574Aspfs*582	✓	—	—
50	III / III	A	1	Int. 38	c.5461-10 T>C	Splice site	—	✓	—
51	III / III	B	2	35	c.4918 C>T	p.Arg1640Trp	✓	—	—
				44	c.6079 C>T	p.Leu2027Phe	✓	—	—
52	III / III	C	1	22	c.3323 G>A	p.Arg1108His	✓	—	—
53	III / III	A	2	Int. 38	c.5461-10 T>C	Splice site	—	—	✓
				47	c.6449 G>A	p.Cys2150Tyr	✓	—	✓
54	III / III	A	2	Int. 38	c.5461-10 T>C	Splice site	—	—	✓
				47	c.6449 G>A	p.Cys2150Tyr	✓	—	✓
55	III / III	A	2	Int. 38	c.5461-10 T>C	Splice site	—	✓	✓
				47	c.6449 G>A	p.Cys2150Tyr	—	✓	✓
56	III / III	D	0				✓	—	—
57	III / III	A	1	**15**	**c.2239delC**	**p.Leu747Cysfs*787**	✓	—	✓
58	III / III	D	0				✓	—	—
59	III / III	C	1	5	c.466 A>G	p.Ile156 Val	✓	—	—

✓ = yes; — = no; APEX = arrayed primer extension microarray; BL = baseline; DS = Sanger direct sequencing; FU = follow-up; Int. = intron; SSCP = single-strand conformation polymorphism.

[a]Putative novel changes are in bold. All the variants are heterogeneous.

SUPPLEMENTAL TABLE 6. Electrophysiologic Group Transition and *ABCA4* Variants[a] Identified in 59 Patients With Stargardt Disease

Pt	Electrophysiologic Group (BL / FU)	Genotype Group	Number of Variants	Exon	Nucleotide Substitution	Amino Acid Change	Screening Method (Yes/No)		
							SSCP	APEX	DS
1	I / I	A	3	6	c.768 G>T	p.Val256Val/ Splice site	✓	✓	—
				17	c.2588 G>C	p.Gly863Ala	✓	✓	—
				19	c.2828 G>A	p.Arg943Gln	—	✓	—
2	I / I	C	1	29	c.4328 G>A	p.Arg1443His	—	✓	—
3	I / I	A	3	**10**	**c.1317 G > A**	**p.Trp439***	—	✓	✓
				17	c.2588 G>C	p.Gly863Ala	—	✓	✓
				43	c.5908 C>T	p.Leu1970Phe	—	✓	✓
4	I / I	C	1	44	c.6079 C>T	p.Leu2027Phe	—	✓	—
5	I / I	A	3	17	c.2588 G>C	p.Gly863Ala	—	✓	—
				19	c.2828 G>A	p.Arg943Gln	—	✓	—
				Int. 38	c.5461-10 T>C	Splice site	—	✓	—
6	I / I	C	1	28	c.4139 C>T	p.Pro1380Leu	—	✓	—
7	I / I	D	0				✓	—	—
8	I / I	B	2	10	c.1253 T>C	p.Phe418Ser	✓	—	✓
				44	c.6079 C>T	p.Leu2027Phe	✓	—	✓
9	I / I	A	2	Int. 28	c.4253+5 G>T	Splice site	✓	✓	—
				30	**c.4519 G > A**	**p.Gly1507Arg**	✓	—	✓
10	I / I	B	2	30	c.4469 G>A	p.Cys1490Tyr	—	✓	✓
				44	c.6089 G>A	p.Arg2030Gln	—	✓	✓
11	I / I	D	0				—	✓	—
12	I / I	C	1	3	c.286 A>C	p.Asn96His	✓	—	—
13	I / I	A	1	30	c.4537_4538insC	p.Gly1513Profs*1554	—	✓	—
14	I / I	D	0				✓	—	—
15	I / I	C	1	46	c.6320 G>A	p.Arg2107His	✓	—	—
16	I / I	D	0				—	✓	—
17	I / I	C	1	3	c.161 G>A	p.Cys54Tyr	✓	—	—
18	I / I	B	2	28	c.4139 C>T	p.Pro1380Leu	—	✓	—
				42	c.5882 G>A	p.Gly1961Glu	—	✓	—
19	I / I	C	1	22	c.3322 C>T	p.Arg1108Cys	✓	—	—
20	I / I	A	2	**10**	**c.1317 G > A**	**p.Trp439***	—	✓	✓
				17	c.2588 G>C	p.Gly863Ala	—	✓	✓
21	I / I	B	3	5	c. 466 A>G	p. Ile156 Val	✓	—	✓
				30	**c. 4363 C > T**	**p. Cys1455Arg**	✓	—	✓
				39	**c. 5516 T > C**	**p. Phe1839Ser**	✓	—	✓
22	I / II	C	1	46	c.6320 G>A	p.Arg2107His	—	✓	—
23	I / II	C	1	17	c.2588 G>C	p.Gly863Ala	—	✓	—
24	I / II	A	1	35	c.4956 T>G	p.Tyr1652*	—	✓	—
25	I / III	A	1	Int. 38	c.5461-10 T>C	Splice site	—	✓	—
26	I / III	D	0				✓	—	—
27	I / III	A	1	22	c.3211_3212insGT	p.Ser1071Cysfs*1084	—	✓	—
28	II / II	A	2	9	c.1222 C>T	p.Arg408*	✓	—	✓
				14	**c.2023 G > A**	**p.Val675Ile**	✓	—	✓
29	II / II	C	1	47	c.6449 G>A	p.Cys2150Tyr	—	—	✓
30	II / II	D	0				—	✓	—
31	II / II	B	3	17	c.2588G>C	p.Gly863Ala	✓	—	—
				22	c.3322 C>T	p.Arg1108Cys	✓	—	—
				19	c.2828 G>A	p.Arg943Gln	✓	—	—
32	II / II	B	2	14	c.1957 C>T	p.Arg653Cys	—	✓	—
				44	c.6089 G>A	p.Arg2030Gln	—	✓	—
33	II / II	D	0				✓	—	—
34	II / II	B	2	17	c.2588 G>C	p.Gly863Ala	✓	—	—
				22	c.3259 G>A	p.Glu1087Lys	✓	—	—

Continued on next page

SUPPLEMENTAL TABLE 5. Detailed Results of Statistical Analysis[a] of Onset of Disease, Duration of Disease, Age at Baseline and Follow-up, Interval of Follow-up, logMAR Visual Acuity, logMAR Visual Acuity Reduction, Yearly Amplitude Reduction, and Yearly Peak Time Shift, With Respect to Electrophysiologic Group at Baseline, Electrophysiologic Deterioration, and Genotype Group

	Electrophysiologic Group at Baseline						Electrophysiologic Deterioration	Genotype Group						
	KW			KW S-D *P* Value			MW *P* Value	MW *P* Value	KW			KW S-D *P* Value			MW *P* Value
Onset of Disease															
χ^2	DOF	*P* Value	Gp1	Gp2	0.326	.155	.034*	χ^2	DOF	*P* Value	GtA	GtB	.091	.038*
14.3	2	.001**	Gp1	Gp3	0.001	.000**		14.3	2	.001**	GtA	GtC	.897	.660
			Gp2	Gp3	0.047	.018*					GtA	GtC	.101	.042*
Duration of Disease														
χ^2	DOF	*P* Value	Gp1	Gp2	.9648		.879	χ^2	DOF	*P* Value	GtA	GtB	.835	
2.2	2	.337	Gp1	Gp3	.3764			3.3	2	.191	GtA	GtC	.247	
			Gp2	Gp3	.4104						GtA	GtC	.312	
Age at Baseline														
χ^2	DOF	*P* Value	Gp1	Gp2	.6044		.283	χ^2	DOF	*P* Value	GtA	GtB	.390	
1.3	2	.521	Gp1	Gp3	.6173			3.3	2	.193	GtA	GtC	.677	
			Gp2	Gp3	.9982						GtA	GtC	.201	
Interval of Follow-up														
χ^2	DOF	*P* Value	Gp1	Gp2	.2904		.272	χ^2	DOF	*P* Value	Gt A	GtB	.921	
5.7	2	.057	Gp1	Gp3	.3833			0.8	2	.668	Gt A	GtC	.627	
			Gp2	Gp3	.0579						Gt A	GtC	.960	
logMAR VA at Baseline														
χ^2	DOF	*P* Value	Gp1	Gp2	.3623	.175	.002**	χ^2	DOF	*P* Value	GtA	GtB	.276	
12.0	2	.003**	Gp1	Gp3	.0029	.001**		3.4	2	.181	GtA	GtC	.261	
			Gp2	Gp3	.0536	.021*					GtA	GtC	.975	
logMAR VA Reduction														
χ^2	DOF	*P* Value	Gp1	Gp2	.7266		.510	χ^2	DOF	*P* Value	GtA	GtB	.938	
1.3	2	.513	Gp1	Gp3	.8456			1.0	2	.605	GtA	GtC	.768	
			Gp2	Gp3	.4994						GtA	GtC	.582	
Yearly Amplitude Reduction for Dark-Adapted 11.0 A-wave														
χ^2	DOF	*P* Value	Gp1	Gp2	.9769	.6153	.013*	χ^2	DOF	*P* Value	GtA	GtB	.042	.0162*
6.3	2	.042*	Gp1	Gp3	.0631	.0248*		7.7	2	.022*	GtA	GtC	.181	.0794
			Gp2	Gp3	.0687	.0272*					GtA	GtC	.201	.0896
Yearly Peak Time Shift for Dark-Adapted 11.0 A-wave														
χ^2	DOF	*P* Value	Gp1	Gp2	.9619		.008**	χ^2	DOF	*P* Value	GtA	GtB	.303	
2.1	2	.343	Gp1	Gp3	.4272			2.4	2	.308	GtA	GtC	.973	
			Gp2	Gp3	.3632						GtA	GtC	.382	
Yearly Amplitude Reduction for Light-Adapted 30 Hz														
χ^2	DOF	*P* Value	Gp1	Gp2	.5895		.407	χ^2	DOF	*P* Value	GtA	GtB	.201	
1.6	2	.450	Gp1	Gp3	.9065			3.6	2	.166	GtA	GtC	.996	
			Gp2	Gp3	.4674						GtA	GtC	.183	
Yearly Peak Time Shift for Light-Adapted 30 Hz														
χ^2	DOF	*P* Value	Gp1	Gp2	.5452	.2969	.000**	χ^2	DOF	*P* Value	GtA	GtB	.617	
5.3	2	.072	Gp1	Gp3	.0708	.0283*		4.7	2	.094	GtA	GtC	.339	
			Gp2	Gp3	.3395	.1634					GtA	GtC	.091	

DOF = degree of freedom; Gp = group; Gt = genotype; KW = Kruskal-Wallis; MW = Mann-Whitney test; S-D = Steel-Dwass.

The Mann-Whitney *U* test was also applied to study the parameters in terms of which the Kruskal-Wallis test detected significant differences between electrophysiologic groups or genotype groups. *for $P < .05$ and **for $P < .01$ are used to identify statistically significant differences.

[a]The Kruskal-Wallis test with Steel-Dwass multiple comparisons was performed to compare the 3 electrophysiologic groups and 3 genotype groups in all combinations. The Mann-Whitney *U* test was applied to investigate the differences between subsets with/without evidence of clinically significant electrophysiologic deterioration.

SUPPLEMENTAL TABLE 4. Detailed Electrophysiologic Findings of 59 Patients With Stargardt Disease: Electrophysiologic Group, Electrophysiologic Deterioration, and Assessment of Each Component of Full-field Electroretinography (*Continued*)

Pt	Selected Eye for Data Analysis	Electrophysiologic Group		Electrophysiologic Deterioration			Dark-Adapted 0.01 (R/L)		Dark-Adapted 11.0 (R/L)		Light-Adapted 30 Hz (R/L)		Light-Adapted 3.0 (R/L)	
		BL	FU	Yes/No	Amplitude Reduction	Peak Time Shift	BL	FU	BL	FU	BL	FU	BL	FU
37	L	2	3	✓	✓	✓	N/N	N/N	N/N	A/A	A/A	A/A	A/A	A/A
38	L	2	3	✓	✓	✓	N/N	A/A	N/N	A/A	A/A	A/A	A/A	A/A
39	R	2	3	✓	—	✓	N/N	NA/NA	N/N	A/A	A/A	A/A	A/A	A/A
40	L	2	3	✓	✓	✓	N/N	A/A	N/N	A/A	N/N	A/A	A/A	A/A
41	R	2	3	✓	—	✓	N/N	A/A	N/N	A/A	N/N	A/A	N/A	A/A
42	L	2	3	✓	✓	—	N/N	A/A	N/N	A/A	A/A	A/A	N/N	A/A
43	L	2	3	✓	✓	—	N/N	A/A	N/N	A/A	A/A	A/A	A/A	A/A
44	R	2	3	✓	✓	✓	N/N	A/A	N/N	A/A	A/A	A/A	A/A	A/A
45	R	3	3	✓	✓	✓	NA/NA	A/A	A/A	A/A	A/A	A/A	A/A	A/A
46	L	3	3	✓	—	✓	NA/NA	N/N	A/A	A/A	A/A	A/A	A/A	A/A
47	R	3	3	✓	—	✓	NA/NA	A/A	A/A	A/A	A/A	A/A	A/A	A/A
48	R	3	3	✓	✓	—	N/N	A/A	N/A	A/A	A/A	A/A	N/N	A/A
49	L	3	3	✓	✓	✓	A/A	A/A	A/A	A/A	A/A	A/A	A/A	A/A
50	R	3	3	✓	✓	✓	A/A	A/A	A/A	A/A	A/A	A/A	A/A	A/A
51	R	3	3	✓	—	✓	A/A	A/A	A/A	A/A	A/A	A/A	A/A	A/A
52	L	3	3	✓	✓	✓	A/A	A/A	A/A	A/A	A/A	A/A	A/A	A/ND
53	L	3	3	✓	✓	✓	A/A	ND/ND	A/A	A/A	ND/ND	ND/ND	ND/ND	ND/ND
54	R	3	3	✓	✓	✓	A/A	ND/ND	A/A	A/A	ND/ND	ND/ND	ND/ND	ND/ND
55	L	3	3	✓	✓	—	A/A	ND/ND	A/A	A/A	A/A	ND/ND	A/A	ND/ND
56	R	3	3	✓	✓	—	A/A	ND/ND	A/A	ND/ND	ND/ND	ND/ND	ND/ND	ND/ND
57	L	3	3	✓	✓	✓	A/A	A/A	A/A	A/A	A/A	A/A	A/A	A/A
58	L	3	3	✓	—	✓	A/A	A/A	A/A	A/A	A/A	A/A	A/A	A/A
59	L	3	3	✓	✓	✓	A/A	A/A	N/A	A/A	N/A	A/A	N/A	A/A

✓ = yes; — = no; A = Abnormal, BL = baseline; Dark-adapted 0.01 = dark-adapted dim flash electroretinogram with flash intensity 0.01 candela second (cd·s)/m^2; Dark-adapted 11.0 = dark-adapted bright flash electroretinogram with flash intensity 11.0 cd·s/m^2; FU = follow-up; L = left; Light-adapted 30 Hz = light-adapted 30 Hz flicker electroretinogram with flash intensity 3.0 cd·s/m^2; Light-adapted 3.0 = light-adapted 2 Hz electroretinogram with flash intensity 3.0 cd·s/m^2; N = normal; NA = not available; ND = not-detectable; Pt = patient; R = right; VA = visual acuity.

SUPPLEMENTAL TABLE 4. Detailed Electrophysiologic Findings of 59 Patients With Stargardt Disease: Electrophysiologic Group, Electrophysiologic Deterioration, and Assessment of Each Component of Full-field Electroretinography

Pt	Selected Eye for Data Analysis	Electrophysiologic Group		Electrophysiologic Deterioration			Dark-Adapted 0.01 (R/L)		Dark-Adapted 11.0 (R/L)		Light-Adapted 30 Hz (R/L)		Light-Adapted 3.0 (R/L)	
		BL	FU	Yes/No	Amplitude Reduction	Peak Time Shift	BL	FU	BL	FU	BL	FU	BL	FU
1	R	1	1	—	—	—	N/N	N/N	N/N	N/N	N/N	N/N	N/N	N/N
2	L	1	1	—	—	—	N/N	N/N	N/N	N/N	N/N	N/N	N/N	N/N
3	L	1	1	—	—	—	N/N	N/N	N/N	N/N	N/N	N/N	N/N	N/N
4	R	1	1	—	—	—	N/N	N/N	N/N	N/N	N/N	N/N	N/N	N/N
5	L	1	1	—	—	—	N/N	N/N	N/N	N/N	N/N	N/N	N/N	N/N
6	R	1	1	—	—	—	N/N	N/N	N/N	N/N	N/N	N/N	N/N	N/N
7	L	1	1	—	—	—	N/N	N/N	N/N	N/N	N/N	N/N	N/N	N/N
8	L	1	1	—	—	—	N/N	N/N	N/N	N/N	N/N	N/N	N/N	N/N
9	R	1	1	—	—	—	N/N	N/N	N/N	N/N	N/N	N/N	N/N	N/NA
10	R	1	1	—	—	—	N/N	N/N	N/N	N/N	N/N	N/N	N/N	N/N
11	R	1	1	—	—	—	N/N	N/N	N/N	N/N	N/N	N/N	N/N	N/N
12	L	1	1	—	—	—	N/N	N/N	N/N	N/N	N/N	N/N	N/N	N/N
13	L	1	1	—	—	—	N/N	N/N	N/N	N/N	NA/N	NA/N	N/N	N/N
14	L	1	1	—	—	—	N/N	N/N	N/N	N/N	N/N	N/N	N/N	N/N
15	R	1	1	—	—	—	N/N	N/N	N/N	N/N	N/N	N/N	N/N	N/N
16	R	1	1	—	—	—	N/N	N/N	N/N	N/N	N/N	N/N	N/N	N/N
17	L	1	1	—	—	—	N/N	N/N	N/N	N/N	N/N	N/N	N/N	N/N
18	L	1	1	—	—	—	N/N	N/N	N/N	N/N	N/N	N/N	NA/N	NA/N
19	L	1	1	—	—	—	N/N	N/N	N/N	N/N	N/N	N/N	N/N	N/N
20	R	1	1	—	—	—	N/N	N/N	N/N	N/N	N/N	N/N	N/N	N/N
21	L	1	1	—	—	—	NA/NA	N/N	N/N	N/N	N/N	N/N	N/N	N/N
22	R	1	2	✓	—	✓	N/N	N/N	N/N	N/N	N/N	A/A	N/N	A/A
23	L	1	2	✓	—	✓	N/N	N/N	N/N	N/N	N/N	A/A	N/N	N/N
24	R	1	2	✓	—	✓	N/N	N/N	N/N	N/N	N/N	A/A	N/N	N/N
25	R	1	3	✓	✓	✓	N/N	N/A	N/N	N/A	N/N	A/A	N/N	A/A
26	L	1	3	✓	—	✓	N/N	N/N	N/N	A/A	N/N	A/A	N/N	A/A
27	L	1	3	✓	✓	✓	N/N	A/A	N/N	N/N	N/N	A/A	N/N	A/A
28	R	2	2	—	—	—	N/N	N/N	N/N	N/N	A/A	A/A	N/N	A/A
29	R	2	2	✓	✓	✓	N/N	N/N	N/N	N/N	N/N	A/A	A/A	A/A
30	L	2	2	—	—	—	N/N	N/N	N/N	N/N	A/A	A/A	N/N	A/A
31	L	2	2	—	—	—	N/N	N/N	N/N	N/N	A/A	A/A	A/A	A/A
32	R	2	2	—	—	—	NA/NA	N/N	N/N	N/N	A/A	A/A	A/A	A/A
33	L	2	2	✓	—	✓	N/N	N/N	N/N	N/N	A/A	A/A	NA/NA	A/A
34	R	2	2	—	—	—	N/N	N/N	N/N	N/N	A/A	A/A	A/A	A/A
35	R	2	2	—	—	—	N/N	N/N	N/N	N/N	A/A	A/A	A/A	A/A
36	L	2	2	✓	✓	—	N/N	N/N	N/N	N/N	A/A	A/A	A/A	A/A

Continued on next page

SUPPLEMENTAL TABLE 3. Primer Sequences and Annealing Temperatures for *ABCA4* Gene Screening

Primer	Sequence (5'–3')	Annealing Temperature (C)
Exon 2 forward	GTGTCTGCTCTGGTTACGTTTTC	61
Exon 2 reverse	CCTTTTGTCTAGAAAGATCTTGGG	
Exon 5 forward	TCCAATCGACTCTGGCTGTT	64
Exon 5 reverse	AGAGATCATGGGGCACAACC	
Exon 9 forward	CCAGCATGGAGTTGAATGAGAC	63
Exon 9 reverse	TAAGTGGACTCTTGCGTTTCCTC	
Exon 10 forward	TTAGATTCTGTCAGCCCAGGAAG	63
Exon 10 reverse	ACCAAGTGGGGTCACTGACTTT	
Exon 15 forward	AGAGAGCCCTTTAGGGCAGAAT	63
Exon 15 reverse	GTTTCCTTGGAAGGGTCCGTAG	
Exon 17 forward	AACTGCGGTAAGGTAGGATAGGG	63
Exon 17 reverse	GACCACCTTTCACAAGTTGCTG	
Exon 30 forward	GCCTAGGGATTTGTCAGCAACT	63
Exon 30 reverse	ACTAAACCAAACTCCCTGCACC	
Exon 38 forward	CCAGTTCACACACATCACCTCAG	63
Exon 38 reverse	ATGAGTGCCACTTTCTTCCTCC	
Exon 39 forward	GTGCTGTCCTGTGAGAGCATCTG	64
Exon 39 reverse	GAGGATTAGGGTGCCTCTGTTTC	
Exon 43 forward	CCCGTGTCAACTGGGACTTAG	63
Exon 43 reverse	ATAGTAGGGTGGCTCTGAGGCC	
Exon 44 forward	GCATTTCTGAAGCCAAATAGGAGA	63
Exon 44 reverse	GTGCATTCTCTTGGAGATGAGAAA	
Exon 46-47 forward	TCTTTACTCTTGGATCCACCTCCT	63
Exon 46-47 reverse	GTGTTCTCCATTGACACTTGGAAG	